Technical Report 2014-8

EVALUATING PACIFIC LAMPREY BEHAVIOR IN FISHWAYS AT BONNEVILLE AND JOHN DAY DAMS USING DUAL-FREQUENCY IDENTIFICATION SONAR (DIDSON), 2013

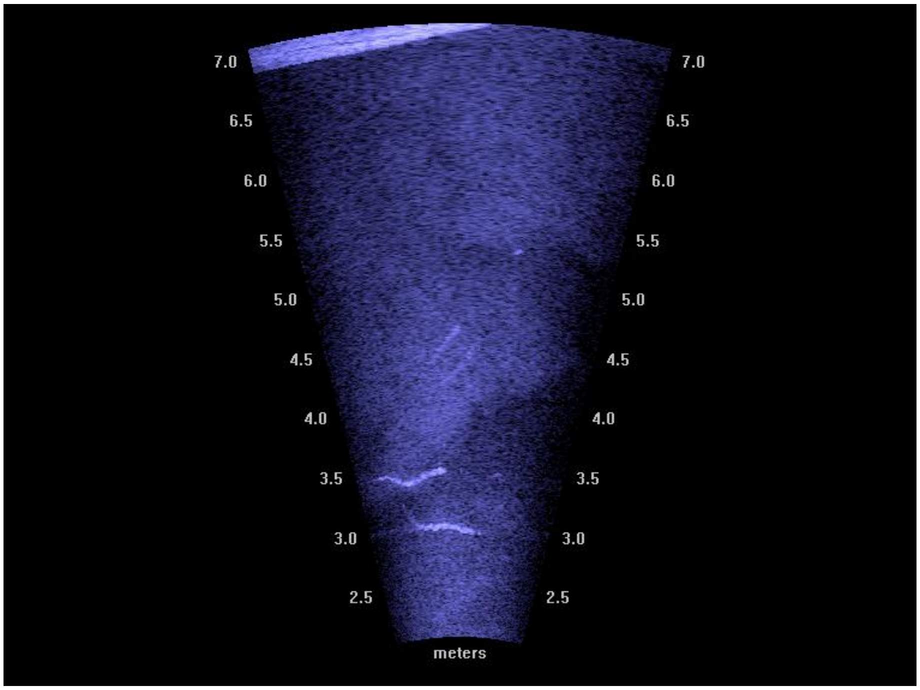

by

M.A. Kirk, M.L. Keefer, and C.C. Caudill
Department of Fish and Wildlife Sciences
University of Idaho, Moscow, ID 83844-1136

for

U.S. Army Corps of Engineers
Portland District

2014

Technical Report 2014-8

EVALUATING PACIFIC LAMPREY BEHAVIOR IN FISHWAYS AT BONNEVILLE AND JOHN DAY DAMS USING DUAL-FREQUENCY IDENTIFICATION SONAR (DIDSON), 2013

by

M.A. Kirk, M.L. Keefer, and C.C. Caudill
Department of Fish and Wildlife Sciences
University of Idaho, Moscow, ID 83844-1136

for

U.S. Army Corps of Engineers
Portland District

2014

Acknowledgements

This project was financed by the U.S. Army Corps of Engineers, Portland District and was facilitated by Sean Tackley. We would like to thank Andy Traylor, Brian Bissell, Ida Royer, Ben Hausman, Miro Zyndol and the additional project biologists at Bonneville and John Day dams. We would like to thank Grant Brink, Kaan Oral, Charles Erdman, Chris Noyes, Eric Johnson, Tami Clabough, Dan Joosten, Steve Lee, Theresa Tillson, Mike Turner, Inga Aprans, and Hattie Zobott from the University of Idaho and William Nagy from the Bonneville Dam Fish Field Unit who provided valuable assistance for this study. The work reported here was conducted under a Cooperative Ecosystems Study Unit (CESU) agreement CESU W912HZ-12-2-0004 with the assistance of Sean Tackley, Glen Rhett, and Deberay Carmichael.

Table of Contents

Executive summary

In 2013, we deployed a Dual-Frequency Identification Sonar (DIDSON) camera at several fishway locations at Bonneville and John Day Dams to observe adult Pacific lamprey (*Entosphenus tridentatus*) behaviors. Our broad objectives were to: 1) evaluate lamprey behavior near the lamprey flume system (LFS) that was installed in the spring of 2013 at Bonneville Dam; and 2) evaluate post-modification lamprey behavior at the John Day north fishway where a bollard field (2012) and a lamprey passage system (LPS, 2013) were recently installed. Additional objectives included determining the lateral and vertical distributions of lamprey in fishways, observing lamprey responses to potential predatory white sturgeon (*Acipenser transmontanus*), and exploring methods for estimating the swim speeds and tail-beat frequencies of lamprey from the DIDSON imagery.

A DIDSON camera was used to monitor different vertical strata of the water column by placing the camera at different depths or by employing an automatic tilting program. The camera was deployed at two locations at Bonneville Dam (Powerhouse 2 north downstream entrance and the Washington-shore junction pool transition area) and at five locations at John Day Dam (three near the north fishway entrance, near the turnpool, and in the transition area). DIDSON images were collected in landscape mode, with the long axis of the sample volume parallel to the ground to obtain information on upstream and downstream movements and to assess horizontal distribution. An automated tilting feature of the DIDSON provided information on the vertical distribution of lamprey in the upper and lower water column. We used a set of morphological and behavioral criteria that were developed in previous years to distinguish adult lamprey from other species.

In total, we collected 457 hours of DIDSON imagery at Bonneville Dam, of which 88 hours were viewed (19% of total collected) using a randomized sub-sampling approach. The majority of lamprey events were at night, reflecting the mostly nocturnal behavior of lamprey during upstream migration. At the Bonneville north downstream entrance (NDE), higher lamprey event rates were observed around the lower LFS entrance slot than at the two upper water column deployments and the proportion of upstream movements was generally high for all NDE deployments. In the Bonneville transition area, lamprey event rates were higher than at NDE and event rates were generally higher in the sample volumes capturing the upper water column. This included higher rates at the overflow weir section versus at the orifice at the second weir in the transition area. It was unclear why lamprey used the upper water column more frequently in the transition area, but two potential mechanisms include avoiding predatory white sturgeon near the fishway floor and inadequate rheotactic (flow) cues for upstream guidance in the lower water column. The horizontal distribution of lamprey in the transition area suggested that upstream movements were relatively equal across the fishway, while downstream movements occurred primarily near the fishway wall. Estimates of lamprey ground speeds did not differ between NDE and the transition area, though water velocity estimates were higher at NDE. Higher tail-beat frequencies were observed at the NDE deployment near the fishway entrance slot, indicating higher lamprey swim speeds through water than in the transition area.

At John Day Dam, we collected 253 hours of DIDSON imagery and viewed 89 hours (35% of the total). The highest event rates were observed at the deployments near the bollard field,

and event rates were higher in sample volumes capturing the lower water column for all deployments. Similar to previous years, we observed more attachment events in the bollard field than at other locations at John Day Dam. Lamprey events were infrequent in the transition area where white sturgeon density was highest, further suggesting that lamprey may be responding to potential predators inside the fishways. The proportion of upstream movements was higher in the lower sample volumes entrance and collection channel deployments, while downstream movements were observed at higher proportions in the upper sample volumes. Lateral distributions of lamprey showed that fish tended toward orientation along the fishway floor in the lower sample volumes and along the fishway wall in the upper sample volumes of the water column.

Our 2013 study expanded upon 2011 and 2012 results by providing new information on Pacific lamprey behavior and exploring new methods for extracting biological information from the DIDSON data. The observations in all years indicate the species may not be as demersal and substrate-oriented as previously hypothesized, particularly in lower velocity environments. Results suggest that Pacific lamprey may respond to hydraulic, biological, and structural cues and that responses differ between low and high velocity sections and in the presence of potential predators. We have also identified potential methods for estimating measures of lamprey *in situ* swimming performance that could provide additional insight into the passage requirements for this species at hydropower dams.

Introduction

Pacific lamprey (*Entosphenus tridentatus*) are a native, anadromous fish in the Columbia River Basin that have experienced considerable declines over the past several decades. Given the cultural and ecological value of the species, increased efforts have been made to identify and remedy the factors causing declines. Large hydropower dams have been identified as a potential causative agent of these declines given the poor passage success of adult lamprey during their upstream migrations (<50%, Moser et al. 2002a, 2002b Johnson et al. 2011; Keefer et al. 2012, 2013b) when compared to the passage of adult salmonids (*Oncorhynchus* spp; >90%, Caudill et al. 2007). Fishways originally designed to facilitate passage of adult salmonids likely contribute to the low passage rates of Pacific lamprey, which differ from salmonids in behavior, swimming mode, and migration ecology.

Radiotelemetry studies have been valuable in identifying the general locations of poor passage within fishways. Areas with poor passage include fishway entrances, collection channels, and transition areas (Moser et al. 2002a, 2002b; Johnson et al. 2012a; Keefer et al. 2013c). Studies conducted in an experimental flume that simulates fishway conditions have also helped identify potential mechanisms of passage failure such as vertical steps, diffuser grating, and high water velocities (Keefer et al. 2010, 2011). However, the spatial scale of radiotelemetry (5-10 m) is often too coarse to identify the specific factors responsible for adult lamprey passage failure. Additionally, the experimental flume studies at relatively small scales may not represent the full range of conditions and behaviors that fish experience or exhibit within the fishway environment. As a result, there is a need for direct behavioral assessments within fishways to identify the relationships between lamprey behavior and the potential reasons for low passage success.

Sonar imaging has provided a non-invasive, imaging tool for effectively monitoring migrations of adult and juvenile fish (Ransom et al. 1996; Steig and Iverson 1998; Pipal et al. 2010; Smith et al. 2010). The high resolution and multi-beam Dual-Frequency Identification Sonar (DIDSON) occupies a niche between short-range optical cameras and low-resolution, long-range (> 10 m) radio- and acoustic telemetry systems. The range that the DIDSON occupies (3-10 m) has been shown to be useful for observational monitoring within fishway environments (Johnson et al. 2011). Although the range of optical video provides a fine enough scale to evaluate Pacific lamprey behaviors at specific locations (e.g., Clabough et al. 2012), it is range limited (<2 m) under low-light or turbid conditions. The DIDSON also has advantages over traditional, single and split-beam echo sounders because it shows the size and general shape of the fish, providing behavioral and species information.

This study summarizes the third year of Pacific lamprey DIDSON observations. The initial application of DIDSON was motivated by a need to employ a non-invasive, monitoring tool to observe lamprey behavior in response to the structural, biological, and hydraulic conditions within fishways. We conducted a pilot study in 2011 to evaluate the feasibility of DIDSON as a sampling tool to monitor adult Pacific lamprey in the Bonneville Dam fishways and found that adult lamprey could be distinguished from other species by their distinctive anguilliform swimming motion. As part of the methods development, we developed additional identification criteria and training protocols for reviewing and scoring lamprey imagery to assess among-viewer consistency of lamprey events, when using multiple viewers to score imagery (Johnson et al. 2012b and *in review*). We expanded upon the 2011 study in 2012 when we deployed the camera at both John Day and Bonneville Dams for site-specific abundance and behavioral evaluations. Results from 2012 demonstrated that lamprey appeared to respond to both biological factors (i.e. presence of white sturgeon, *Acipenser transmontanus*) and structural modifications (i.e. bollard field at John Day) within fishways (Johnson et al. 2013).

Study locations selected in 2013 included new and previously used sites at Bonneville and John Day dams. The 2013 Bonneville study sites included new locations at the north downstream entrance (NDE) to the Washington-shore fishway and the Washington-shore transition area upstream of the junction pool (JPU). At John Day, the DIDSON was deployed at a series of locations inside the north fishway entrance and collection channel. Objectives for 2013 at Bonneville Dam included:

1) observing general behavior of adult lamprey at the recently installed Lamprey Flume System (LFS) at NDE;

2) identifying associations between lamprey and white sturgeon activity in the transition area;

3) identifying vertical distribution of lamprey in the transition area near the second overflow weir; and

4) estimating lamprey ground speeds and tail-beat frequencies at NDE and in the transition area.

Objectives at John Day were similar to those in 2012 and included:

1) evaluating lamprey behavior near the bollard field at the fishway entrance;

2) evaluating the vertical and lateral distribution of fish as they exited the bollard field;

3) evaluating lamprey distribution in relation to the recently installed lamprey passage system (LPS); and

4) determining the distribution of lamprey through the collection channel

Methods

The DIDSON was developed by the University of Washington's Applied Physics Laboratory (Belcher et al. 1999, 2001; Tiffan et al. 2004) and uses a high resolution acoustic lens to produce images of the underwater environment. It is conventionally used where underwater cameras would be limited by low light levels and/or high turbidity. In past studies, the images within 8-10 m of the sonar camera were of high enough resolution to identify fish orientation, heading, and movement direction (Moursund et al. 2003; Holmes et al. 2006). The multibeam nature of the DIDSON makes it robust in the acoustically noisy environments commonly encountered at hydropower facilities and the operating frequencies are beyond the range that would affect fish behavior (Fay and Simmonds 1999).

DIDSON deployment and set-up

The DIDSON 300 M sonar camera (Sound Metrics Corp., Bothel, WA) we used consisted of a transducer array and acoustic lens that generated real-time acoustic images that were transmitted to a topside control box using an underwater telemetry cable. A laptop was used to control the DIDSON settings, orient the position of the DIDSON, and record data. The DIDSON camera was mounted to a 2-axis X2 Rotator (Sound Metrics Corps, Bothel, WA) that allowed the operator to remotely pan and tilt the camera using laptop computer controls. The DIDSON sonar and rotator were mounted to an aluminum trolley that was deployed onto steel I-beams at each deployment location and retrieved using a Thern Series 5122 portable davit crane. The laptop computer, DIDSON topside control box, and battery backup were housed in waterproof storage units situated near the I-beams. A 1 TB removable storage drive (Western Digital) was used to transfer data to a larger 10 TB network drive (Netgear Ready NAS) for continuous data storage. High resolution video files were saved in 10-min increments to facilitate data management and the data review process. The frame rate was set to 10 frames per second, which provided adequate resolution to identify the unique shape and swimming motion of lamprey from other targets.

Sonar orientation and tilting program

We deployed the camera in high frequency mode (1.8 MHz) as it provided higher resolution images that allowed us to distinguish the shape, movement, size, and orientation of adult lamprey. In the high frequency mode, the DIDSON produces 96 acoustic beams with each beam 0.3° in the horizontal direction and 14° in elevation. This resulted in a total sample volume of 29° (horizontal) x 14° (vertical) (Figure 1). The sonar was generally positioned to sample perpendicular to the flow and imaged a lateral (side) view of the fish, although various deployments positioned the DIDSON to sample a volume parallel to flow. The specific direction and orientation of the DIDSON varied based upon both the deployment location and the specific objectives of that deployment. We found it useful to have some fishway structure in the field of view as reference for confirming the camera placement and determining the fish's orientation and swimming direction.

All of the monitoring in 2013 was conducted with the DIDSON in 'landscape mode.' This configuration orients the camera so that the pan axis of the rotator positioned the camera along the horizontal plane and the 29° component of the sample volume spread laterally. Landscape mode provides information on the upstream and downstream movements of fish, as well as the distance of fish from the camera (range). In previous years, we also deployed the DIDSON in 'portrait mode', which provides information on the depth of fish within the sample volume by capturing a "side-view" or elevation view of the sample area. However, we found that lamprey were more difficult to distinguish in portrait deployments, and in 2013 chose to use tilting programs with the camera in landscape mode to make inferences about the vertical distribution of lamprey in the water column. All of the selected locations allowed us to image approximately 15%-50% of the fishway channel in the vertical plane and the frame of view spanned the entire channel width at most locations. Data collection parameters normally included a sample window start of 2 m and a window length of 5-6 m.

For each deployment, the camera sampled either a single fixed sample volume ("FIXED" deployments) or two sample volumes capturing two vertical strata of the same approximate horizontal area ("TILT" deployments, e.g., Figure 1). The TILT deployments used an automated tilting program of the DIDSON X2 Rotator to alternate imaging between upper and lower sample volumes every 10 minutes. The TILT deployments provided direct comparison of distributions within the upper vs. lower sample volumes during a single ~24 sampling period with similar conditions (e.g., similar densities of adult lamprey, tailrace elevation, etc.). Some deployments at Bonneville could not use the tilting feature due to mechanical issues with the Rotator, and thus only sampled one stratum of the water column, which were denoted as having a FIXED orientation. Similarly, some locations included a mix of TILT and FIXED deployments, and where appropriate, orientations were combined across nights. The criteria for combining TILT and FIXED deployments included: 1) deployments with similar imagery; 2) similar deployment details (depth, tilt, compass direction, etc.); and 3) occurring within the major period of the run season (i.e. early June to late July). We note that the FIXED terminology used here differs from the VERT deployments used in 2011-2012. In both, the camera was deployed in a landscape orientation at a fixed angle position. However, the VERT deployments in 2011-2012 alternated a horizontally oriented camera among two or more depths across several sequential nights to estimate depth distribution at a single location, whereas the FIXED deployments used in 2013 were at a single depth and camera angle.

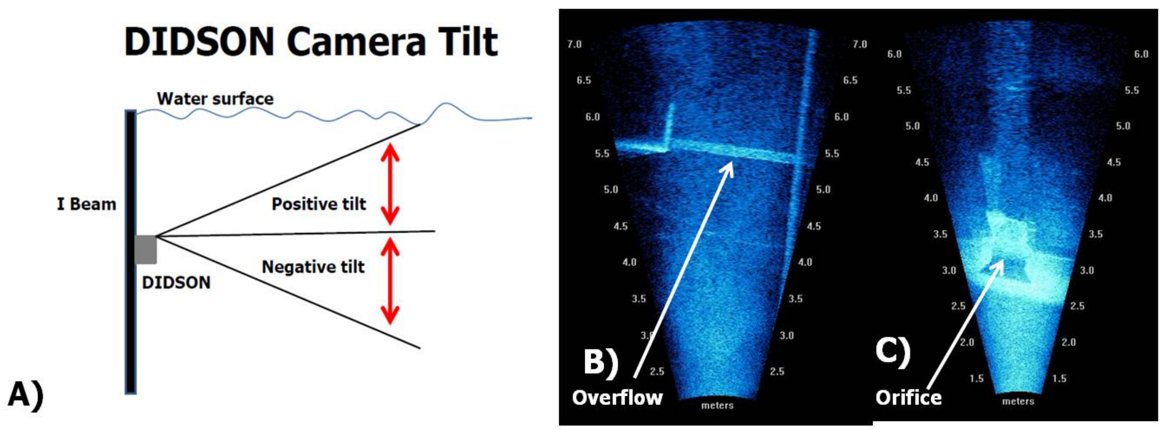

Figure 1. An example of the DIDSON sample volumes captured in the negative and positive tilt at the transition area site at Bonneville: A) Orientation of the DIDSON and sample volumes collected (represented by red arrows) in the water column when the camera would alternate between positive and negative tilts. Alternating the camera between these positive and negative tilts allowed us to evaluate behavior in both the upper and lower water column within the same deployment, such as at the (B) overflow and (C) orifice sections of an overflow weir in the transition area imaged at JPU_SHORT.

Deployment locations at Bonneville and John Day Dams

There were two sampling locations at Bonneville Dam and both were located in or near the Powerhouse 2 (PH2) fishway on the Washington shore (Figure 2). The first location was at the PH2 north downstream entrance (NDE), which underwent entrance modifications via the installation of the lamprey flume system (LFS) in the spring of 2013. Deployments were made orienting the camera both upstream (NDE_UP) and downstream (NDE_DOWN) in the upper water column, to evaluate movement through a typical fishway entrance (UP) and during approach (DOWN: Figure 2B). Two slightly different deployments were made orienting the DIDSON at the LFS with one deployment in the lower water column with a side view of the LFS entrance slot (NDE_LFS_LOW) and one in the upper water column (NDE_LFS_UP) with a top-down view of the entrance slot. Deployments at NDE were limited due to high velocities and damage suffered to the camera. Deployments were conducted from 20 June to 7 July, 16-21 July, 30-31 July, and 27 August to 2 September. Appendix A contains a comprehensive list of the specific deployment dates, deployment details, and images of camera orientations for Bonneville and John Day dam locations.

The second location at Bonneville Dam was at the PH2 transition area/junction pool (JPU) at the location of the first and second weir of the fish ladder (referred to Weir 8 and 9 based on elevation above sea level; Figure 2). These weirs are fully submerged through the fish passage season and have been hypothesized to impede passage. Three deployments were made using the tilting programs that could orient the DIDSON to different portions of the water column. The first oriented the camera towards the far side of the submerged second overflow weir in the negative tilt and along the south fishway wall in the positive tilt (JPU_LONG; Figure 2C). The second was oriented to the near side of the second overflow weir on the north wall aimed at the overflow (positive tilt) and orifice (negative tilt) sections (JPU_SHORT; Figure 2E). The third deployment aimed across the fishway looking above (positive tilt) and below (negative tilt) the first overflow weir (JPU_XSECT; Figure 2D). In addition, two late-season deployments (30-31 August and 31 August to 1 September) were made at JPU_SHORT to evaluate potential differences in lamprey behavior within the transition area at lower tailwater elevation. An additional late-season deployment occurred at JPU_XSECT (27-29 August) that was not consistent with previous deployments and was considered an independent deployment (JPU_XSECT_LATE). Rather, imagery was similar to the JPU_LONG deployment with a negative tilt capturing the lower water column and the south fishway wall (but not the fishway floor).

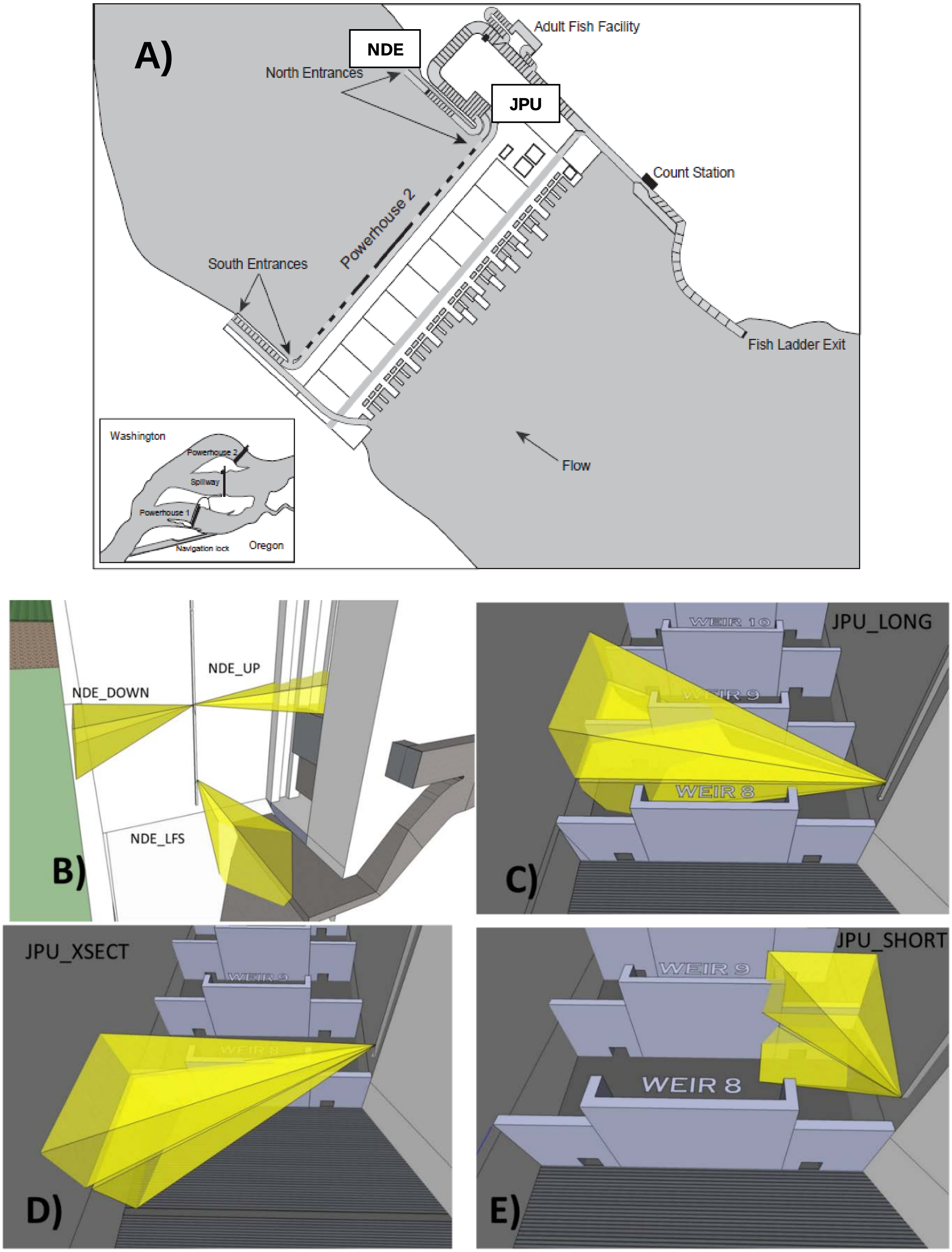

Figure 2. Location of DIDSON observations at Bonneville Dam Powerhouse 2 during 2013 (Panel A). Observations were made at the North Downstream Entrance (NDE; Panel B) of the Washington-shore fishway and the upper junction pool/lower transition area (Panels C-D). See Appendix A for additional details and photos.

We deployed the camera from 9-15 July and 22-28 July at five different sampling locations in the lower section of the north fishway at John Day Dam (Figure 3; see Appendix B for photographs also). Two deployments were within the collection channel (JD1, JD3) along the north wall and were cross-sectional views aimed directly across the fishway to evaluate lamprey lateral and vertical distribution. Another cross-sectional deployment (JD4) was just downstream from the first overflow weir along the south wall in the transition area. Two sites (JD5 and JD6) were along the south fishway wall near the fishway entrance. Two orientations at the JD5 site were oriented across the fishway channel to evaluate how lamprey exited the bollard field (JD5_XSECT) and to image lamprey behavior at the recently installed lamprey passage system (JD5_LPS). The final deployment site (JD6) was on a slanted I-beam directly next to the JD5 site to assess lamprey use of the bollard field.

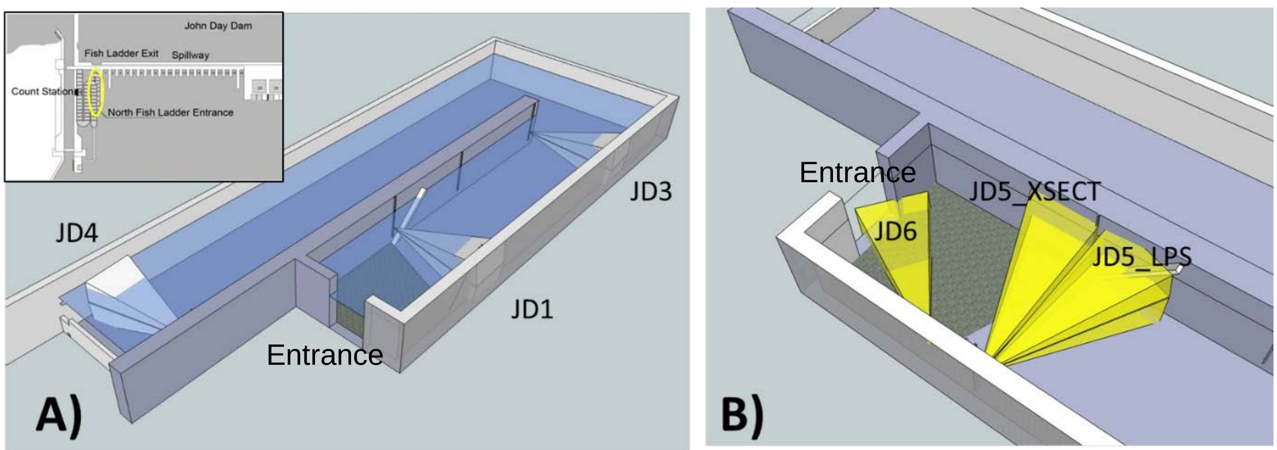

Figure 3. Locations of the five I-beams where the DIDSON was deployed in the lower north fishway of John Day Dam in 2013. See Appendix A for additional details and photos.

Data review and analysis

Video files were processed by trained University of Idaho fisheries personnel using DIDSON v5.25.25 software. We have previously established four identification criteria and a reviewing protocol that were used to classify targets as adult lamprey versus other species (Johnson et al. *in review*):

1. anguilliform swimming motion (Breder 1926), as opposed to subcarangiform motion of salmonids (*Oncorhynchus* spp.) and American shad (*Alosa sapidissima*). In particular, the wavelength relative to the body length of swimming lamprey was shorter in lamprey than in salmonids or shad. A full waveform was often visible in lamprey but only one half a waveform was visible in salmonids and shad. In other words, lamprey frequently appeared s-shaped with a snake-like swimming motion, while salmonids and shad appeared c-shaped.
2. target shape, including length:width ratio and lack of protruding fins.
3. target size of ~50-80 cm.
4. other characteristic lamprey behaviors such as attachment to surfaces.

We developed a sampling design and reviewing protocol in our 2011 pilot study to standardize lamprey identification and scoring of DIDSON files that we continued to use in the 2012 and 2013 studies. We used random subsampling to select files for review given the high volume of data collected throughout the field season. A data manager, who was also a reviewer selected the subsampled files and randomly distributed them among the reviewers. Aside from a subset of random "multi-viewer files" (~10% of review files), most files were only watched by one reviewer. The *a priori* subsampling scheme favored night-time files over day-time files due to the primarily nocturnal behavior lamprey exhibit in their upstream migrations (~2:1 ratio). We attempted to watch a relatively equal proportion of video from each of the deployments (Table 1).

To help standardize the review process, inexperienced viewers independently watched and scored lamprey events from a common set of training files prior to data collection. Viewers then reviewed the common files and event scoring with an experienced DIDSON technician. This training exercise helped to produce the lamprey identification criteria listed above. To control for among-viewer variability that may occur in lamprey identification, reviewers assigned a confidence level (low, medium, high) to each lamprey event. 'High' confidence was assigned to events that met most or all of the lamprey identification criteria. 'Medium' confidence was assigned to events that met more than one of the identification criteria, and 'low' confidence was assigned to events that were potentially lamprey but had few conclusive characteristics. These confidence ratings were necessarily qualitative given that context-specific challenges existed that created variability in the image quality. These challenges included the length of time that lamprey were in the field of view, the number of other fish present, and image differences related to the deployment type and orientation of lamprey to the camera.

Once a target was identified, we used tools in the DIDSON v5.25.25 software to measure the image distance from the camera (defined as range) and image location in the horizontal plane with respect to the camera (defined as angle). Range and angle were recorded for the first and last image of each individual lamprey event. Viewers also recorded lamprey orientation (i.e., facing upstream or downstream), whether the lamprey attached its oral disc to any substrate, where that attachment occurred, and details of the DIDSON file (filename, site, date, review rate [frames/sec]). Review rates ranged from 10-12 frames/sec. Data for each event were entered into individual spreadsheets and events recorded by all viewers were compiled into a master database for analyses. The determination of whether fish were moving upstream or downstream was calculated by subtracting either the angle or range (depending upon camera orientation with respect to the flow) from the first observation of the fish and the last observation of the fish.

During the review process of all camera deployments, we scored an index of white sturgeon activity. The index was a relative measure only and was calculated by counting the number of white sturgeon sightings per ten minute file. A sighting was defined as when a sturgeon came into the frame of view until the time it exited the field. The index thus should not be considered a measure of abundance since it likely overestimates the number of unique sturgeon (i.e., individuals were counted more than once); rather, it should be considered as an estimation of sturgeon presence or activity. An hourly index score was calculated as a measure of sturgeon sightings per hour.

Table 1. Total number of hours of DIDSON imagery collected and number of hours watched at the different deployment locations in 2013 at Bonneville and John Day Dams. Orientation: TILT = tilting feature to capture more than one depth strata, FIXED = capturing one depth stratum. NDE and JPU sites were deployments at Bonneville Dam.

		Data collected (h)			Data watched (h)			Data watched (%)		
Site	Orientation	Day	Night	Total	Day	Night	Total	Day	Night	Total
NDE_LFS_UP	FIXED	6.3	7.2	13.5	2.8	6.2	9.0	44.4	86.1	66.7
NDE_LFS_LOW	FIXED	19.7	14.8	34.5	3.6	7.0	10.6	18.3	47.3	30.7
NDE_DOWN	FIXED	17.5	8.5	26.0	3.8	7.7	11.5	21.9	90.3	44.2
NDE_UP	FIXED	3.0	8.5	11.5	2.7	6.7	9.3	89.0	78.5	81.2
JPU_LONG	FIXED/TILT	52.3	46.5	96.8	5.3	10.3	15.6	10.2	22.2	16.2
JPU_SHORT	FIXED/TILT	97.4	61.3	158.7	7.8	14.2	22.0	8.0	23.1	13.9
JPU_XSECT	FIXED/TILT	74.1	42.5	116.6	3.2	7.2	10.3	37.3	66.7	49.2
JD1	TILT	16.3	8.5	24.8	4.0	6.0	10.0	61.3	70.6	40.3
JD3	TILT	12.5	8.5	21.0	4.7	5.7	10.3	37.4	66.7	49.2
JD4	TILT	40.5	25.5	66.0	6.8	13.3	20.2	16.9	52.3	30.5
JD5_XSECT	TILT	27.9	17.0	44.9	3.2	6.5	9.7	11.4	38.2	21.5
JD5_LPS	TILT	9.7	8.5	18.2	3.0	4.8	7.8	31.0	56.8	43.0
JD5_FIXED	FIXED	24.2	17.0	41.2	3.0	7.0	10.0	12.4	41.2	24.3
JD6	FIXED/TILT	19.4	17.0	36.4	8.2	12.7	20.8	42.1	74.5	57.3

Among-viewer comparison: Quality control evaluation

In addition to the common set of training files, we compared the consistency of scoring among viewers using a set of "multi-viewer" files that were watched by all DIDSON reviewers. These files were randomly selected from the subsample described above and were distributed randomly throughout the viewing period. One reviewer (the data manager) knew which DIDSON files were multi-viewer files and was solely responsible for assigning the files. Reviewers with the exception of the data manager were unaware of the time or date for individual files within location. We used the data to compare the total number of events scored per viewer, event confidence agreement among viewers, and event identification agreement among viewers. The agreement metrics were calculated by comparing scores and confidence levels for individual events for all pairs of viewers. Event agreement was expressed as the percentage of the events scored by both viewers in each pair (i.e., if both viewers scored the event then their agreement was 1, and if only one viewer scored the event then agreement was 0); event confidence level was not considered, but all scored events were included. Similarly, confidence level agreement was the percentage of events scored with medium or high scores or high scores only.

Lateral distribution estimates

When the DIDSON sample volume spanned the entire fishway channel at a particular deployment, estimating lamprey distance from the camera (range) allowed us to develop inferences regarding the lateral distribution of lamprey across the channel. However, because the DIDSON field of view increased with increasing distance from the camera, the probability of capturing lamprey images increased with distance as well (Figure 1). We therefore weighted our estimates of the number of events in each range segment (bin) by the volume of the observed area in 0.5 m long increments, as measured from the camera. The geometric formula we used to calculate volume was for a ‘truncated rectangular pyramid’:

$$\text{Volume} = (1/3*H)*(A*B + \text{sqrt}[A*B*C*D] + C*D)$$

where H = the bin width (i.e., 0.5 m increments in distance from camera), A = width at the near end of the bin, B = height at the near end of the bin, C = width at the far end of bin, and D = height at the far end of the bin. We believe that the unweighted observational data, in combination with the weighted estimates, capture the likely range of the lateral distributions of lamprey.

Water velocity and lamprey ground speed estimates

A new study component to this year’s study was to evaluate the potential of DIDSON data for making estimates of lamprey swim speed, as has been estimated using DIDSON for other species (Mueller et al. 2008, 2010). We estimated both ground speed and swim speed through water, and estimates were primarily done as an exercise to consider the precision and potential future application of these methods. To calculate ground speed, we used the measuring tool in the DIDSON v5.25.25 software to measure the distance individual fish swam divided by the number of frames (time) it took for fish to swim that distance. We then estimated swim speed through water by combining ground speeds and estimates of water velocity. Water velocity estimates were calculated similarly except that estimates were based on the distance that individual suspended particles traveled in the flow field, assuming the particles were transported passively. Ten estimates of particle velocity were made for each video file and the average of those ten estimates was the estimated mean water velocity for that file. Given the uncertainty in the precision of these estimates, comparisons were made to sources of known hydraulic estimates regarding velocities at some locations to corroborate our estimates. We assumed that water and fish were traveling parallel (coplanar) to the horizontal axis of the DIDSON sample volume, and thus reported estimates represent minimum estimates. The speed through water of individual fish was calculated as

$$\text{Swim speed through water} = \text{ground speed} - \text{mean water velocity}$$

where upstream velocities were positive (e.g., lamprey movement) and downstream velocities were negative (e.g., water velocities).

Tail-beat frequency estimates

A second estimate of lamprey swimming capacity was tail-beat frequency (TBF). TBF describes the rate at which fish undulate their body to generate swimming thrust and power. It has been used as a measure of swimming performance that correlates with fish energetic expenditure (Standen et al. 2002; Steinhausen et al. 2005). We followed a method developed by Mueller et al. (2010) for estimating TBFs from the echogram procedure available in the

DIDSON v5.25.25 software. The echogram collapsed all of the range samples from a specific time frame into a single column of data. The echogram then plots the maximum intensity of the DIDSON's 96 acoustic beams for each range on a vertical axis for each specific time frame. The maximum intensity of the tail undulation is visually represented either as a series of convex and concave humps or as "spikes" on the echogram, depending upon the orientation of the fish to the camera. These spikes correspond to a specific position of the tail in the swimming motion of the fish, thus providing details about the rate of tail-beats (or body undulations) for individual fish. Figure 4 provides a visual explanation of this process.

Following the methods of Mueller et al. (2010), the TBF of an individual fish was calculated with the equation:

$$\mathrm{TBF} = \frac{(n-1)}{\sum_{i=1}^{n-1}(t_i + 1 - t_i)}$$

where n is equal to the number of peaks and t_i is the time of each individual peak. Time t represents the time interval between peaks (i.e. shorter time differences between peaks generates higher estimates of TBF).

A number of restrictions were placed on the lamprey selected for swim speed and TBF estimates. First, we only included those classified by reviewers as medium or high confidence events. Second, we restricted estimates to fish that had an upstream orientation. Third, we estimated ground speeds for fish that had a roughly linear swim path. Fourth, water velocity, ground speed, and TBF estimates were only made for deployments in the upper water column, because the acoustic reflection on the fishway floor can mask the flow fields and any moving particles. Fifth, for the TBF estimates, fish needed to have at least four consecutive discernible "spikes" in the echogram. Lastly, all estimates reported here were from lamprey detected at the NDE and JPU locations at Bonneville Dam.

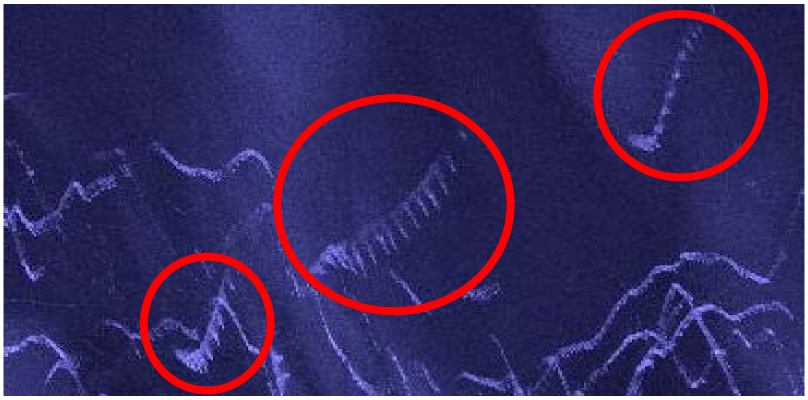

Figure 4. Example of tail-beat frequency (TBF) patterns generated from the echogram procedure in the DIDSON v5.25.25 software. The y-axis depicts range (distance from camera) and the x-axis represents time (frame number). Brightness indicates intensity of reflected acoustic signals. The echo traces of three lamprey from the JPU_LONG deployment are shown in this figure (enclosed by red circles). The "spikes" in each example represent the position of the lamprey's body as it undulates from side to side. The time difference between the peaks of each successive spike provides information about the rate at which the body is undulating. The greater the time between peaks, the shorter the TBF estimate.

Results

Among-viewer comparison – Bonneville Dam

A total of 48 (6.0 h) DIDSON files were watched by five reviewers (Table 2). Between 0 and 49 total lamprey events were scored in each of the ten deployments. The highest number of total events, events/viewer, and events/h were recorded in the JPU_XSECT tilting deployment. Three or fewer events were scored in the JPU_LONG tilting and two of the NDE deployments.

The number of events scored per viewer varied widely within deployments. For example, the five viewers scored between 2 and 11 events at the NDE_DOWN deployment (Table 2). The coefficient of variation (CV = standard deviation/mean) for the number of events at NDE_DOWN was 44%. There was higher agreement at JPU_XSECT, where viewers scored between 27 and 37 events (CV = 16%), and at JPU_SHORT (*range* = 36-35, CV = 15%). Other deployments had relatively few event observations.

Event identification agreement for the 10 pairs of viewers ranged from a median of 28% in the combined NDE files to a median of 60% in the combined JPU files (Figure 5). At all sites, viewer event agreement increased as confidence level increased. For example, in the NDE files median among-viewer event agreement for the 10 viewer pairs was 28% when all confidence levels were included, increased to 38% when only medium and high confidence events were included, and was 63% when only high confidence events were included. Notably, only a small percentage of lamprey events were scored by all five viewers in any deployment. In the combined NDE files, for example, only 2 (7%) of 28 lamprey events were identified by all viewers. The percentage of events identified by all five viewers in the JPU deployments was 39% (Figure 6).

Among-viewer comparison – John Day Dam

A total of 50 (6.3 h) DIDSON files were watched by five viewers (Table 2). Between 5 and 26 total lamprey events were scored in each of the deployments that primarily monitored swimming fish. Many additional events were scored in the bollard field deployments, but these were difficult to match and enumerate across viewers due to extended attachment events. In the non-bollard deployments, the highest number of total events, events/viewer, and events/h were recorded in the JD5_XSECT deployment. In the bollard deployments, individual viewers scored up to 34 events (JD6_TILT, Table 2).

As in the Bonneville evaluation, the number of events scored per viewer varied considerably within John Day deployments. In fact, coefficients of variation were generally higher at John Day than at Bonneville, in part because the total numbers of events per deployment were small (including zero events for some viewers at some deployments; Table 2).

Across all non-bollard deployments at John Day Dam, event identification agreement for the 10 pairs of viewers was 38% (*median*) for 54 events (Figure 5). Median agreement increased to 50% when only medium and high confidence events were included and to 58% for high confidence events. Of the 54 non-bollard field lamprey events scored at John Day, 6 (11%) were scored by all seven viewers (Figure 7).

Scoring rates (events/h) in the bollard field deployments were moderately consistent across viewers. It was difficult to match individual events because some lamprey were present for extended periods and the first observation times often differed among viewers. Nonetheless, in the deployment with the most observations (JD6_FIXED) the number of scored events ranged from 24-34 per viewer (CV = 13%; Table 2), similar to the free swimming observations in other deployments. The spatial distribution of the attachment events was qualitatively similar among viewers.

Table 2. Summary of the files reviewed in the multi-viewer quality control evaluation. Total events are the number of unique lamprey events of all confidence levels, with all viewers' scoring combined.

Site	Orientation	Dates	View time (min)	Total events	Events/viewer Mean	Events/viewer Range	Events/h Mean	Events/h Range
Bonneville								
JPU_LONG	TILT	1	10	0	-	-	-	-
	FIXED	2	50	7	5	3-6	5.8	3.6-6.0
JPU_SHORT	TILT	4	60	47	30	26-35	29.6	26.0-35.0
	FIXED	2	50	2	<1	0-1	0.5	0.0-1.2
JPU_XSECT	LATE*	4	60	11	7	5-10	7.2	5.0-7.0
	TILT	2	60	49	34	27-41	34.2	27.0-41.0
NDE_DOWN	FIXED	2	50	19	8	2-11	9.6	2.4-13.2
NDE_LFS_UP	FIXED	1	30	5	3	1-4	5.2	2.0-8.0
NDE_LFS_LOW	FIXED	2	60	1	1	1-1	1.0	1.0-1.0
NDE_UP	FIXED	1	50	3	1	0-2	1.0	0.0-2.4
John Day								
JD1	TILT	2	60	5	3	1-5	2.8	1.0-5.0
JD3	TILT	2	100	11	5	0-10	3.2	0.0-6.0
JD4	TILT	4	90	5	1	0-2	0.7	0.0-1.3
JD5_XSECT	TILT	2	70	26	15	11-23	12.5	9.4-19.7
JD5_LPS	TILT	2	50	8	2	1-4	2.9	1.2-4.8
JD5_FIXED	FIXED	3	60	n/a	5	2-7	7.8	3.0-10.5
JD6	TILT	1	30	n/a	3	1-5	6.8	2.0-10.0
	FIXED	2	40	n/a	28	24-34	42.3	36.0-51.0

* This was the late season deployment that was not consistent with the other JPU_XECT deployments.

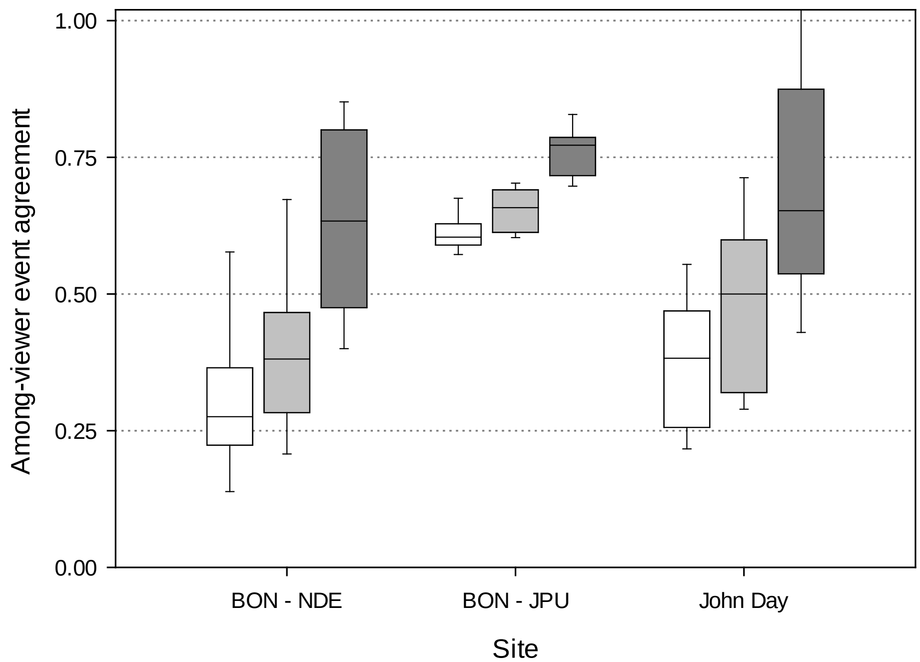

Figure 5. Among-viewer (n = 5) agreement on lamprey event identification. Box plots (5th, 10th, 25th, 50th, 75th, 90th, and 95th percentiles) show agreement for 10 pairs of viewers at each site (multiple deployments combined per site). White boxes include all low, medium and high confidence events. Light grey boxes: all medium and high events. Dark grey boxes: high events only. Note that event agreement increases with viewer confidence.

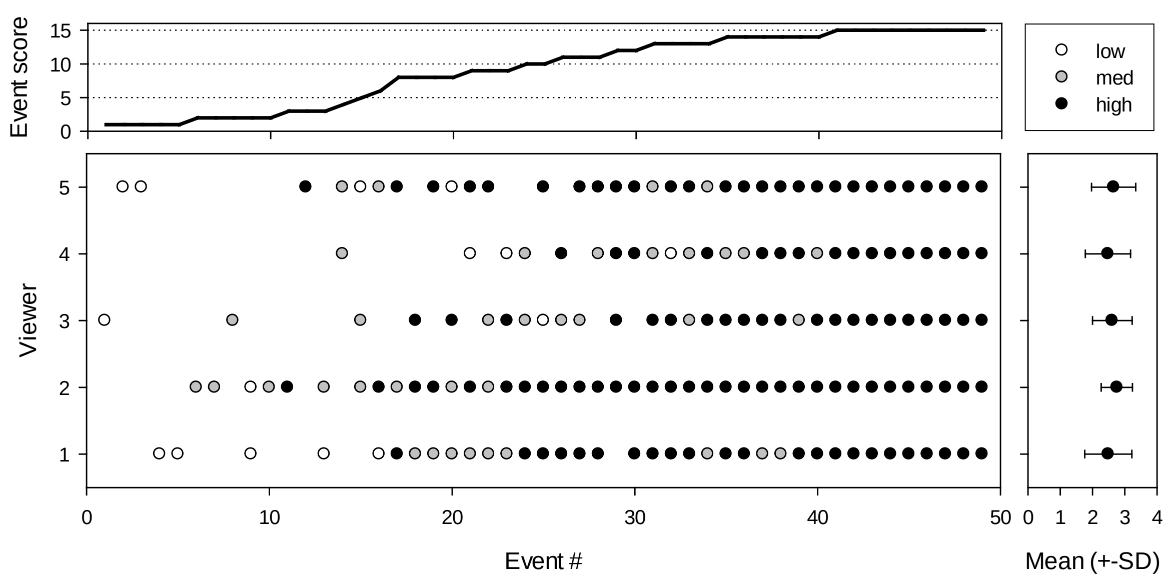

Figure 6. Lamprey event scoring by five reviewers at the Bonneville transition pool (JPU_XSECT) collected during 60 minutes ordered by total score. Scores were: 1 for low (○), 2 for medium (●), and three for high (●) confidence. Top panel shows the total score for each event (n = 49), including 19 (39%) that were identified by all viewers.

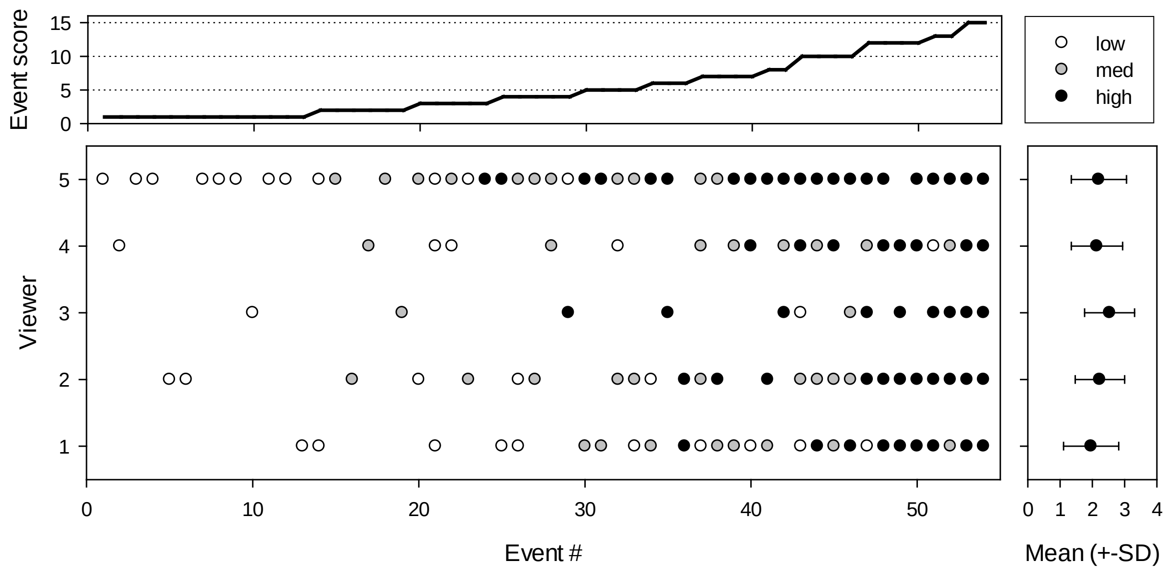

Figure 7. Lamprey event scoring by five reviewers at the John Day deployments (JD1, JD3, JD4, JD5_XSECT) collected during 370 minutes ordered by total score. Scores were: 1 for low (○), 2 for medium (●), and three for high (●) confidence. Top panel shows the total score for each event (n = 54), including 6 (11%) that were identified by all viewers. (Note: does not include attachment events observed in the bollard field.)

Bonneville Dam

Bonneville Dam: Event rates and confidence levels

At Bonneville Dam, we observed a total of 1,325 lamprey events with 1,073 of those recorded in the JPU deployments (Table 3). Nearly all (1,299) events were at night (2100-0530) with only 26 events observed in daytime files. Event rates varied considerably between the different deployment locations. JPU sites had more events per hour than the NDE sites with the highest nighttime event rate at the JPU_XSECT deployment (86.4/h) and the lowest nighttime event rate at NDE_DOWN (5.4/h) (Figure 8). At the NDE deployments, nighttime event rates were highest for the NDE_LFS_UP deployment (20.9/h). Slightly lower event rates were observed at the NDE_UP (9.3/h) and NDE_DOWN (5.4/h) deployments. The highest event rate in the daytime files was at JPU_XSECT (4.1/h). We observed no lamprey attached to any surfaces in the Bonneville deployments.

Confidence levels also differed among deployment locations (Table 3). The highest proportion of events that were observed at the JPU deployments were classified as high confidence (deployment range: 0.64-0.76). In contrast, the proportion of high confidence events was much lower at NDE (range: 0.25-0.53), and the proportion of low confidence events were higher for NDE (range: 0.15-0.40) compared with JPU (range: 0.05-0.14) (Figure 9). Given that few daytime events were observed and the limited conclusions that we could draw from them, all daytime events and files were excluded from the remaining analyses.

Table 3. Number of files, hours, events, and distribution of events based upon confidence level for all Bonneville and John Day deployments in 2013. Note that FIXED and TILT files were combined because those orientations had similar imagery and deployment characteristics.

Deployment site	Orientation	Number Files	Hours Watched	Number Events	Confidence levels (%) H	M	L
NDE_LFS_UP	FIXED	54	9.00	134	71 (53%)	45 (33%)	19 (14%)
NDE_LFS_LOW	FIXED	64	10.67	15	6 (43%)	5 (33%)	4 (26%)
NDE_DOWN	FIXED	69	11.50	40	10 (25%)	14 (35%)	16 (40%)
NDE_UP	FIXED	56	9.34	63	29 (46%)	19 (30%)	15 (24%)
JPU_LONG	TILT/FIXED	94	15.66	386	292 (76%)	75 (19%)	19 (5%)
JPU_SHORT	TILT/FIXED	132	22.00	116	85 (73%)	19 (16%)	12 (11%)
JPU_XSECT	TILT/FIXED	62	10.34	671	427 (64%)	148 (22%)	96 (14%)
JD1	TILT	60	10.00	35	18 (51%)	7 (20%)	10 (29%)
JD3	TILT	62	10.34	88	57 (65%)	21 (24%)	10 (11%)
JD4	TILT	121	20.16	11	2 (18%)	5 (45%)	4 (37%)
JD5_XSECT	TILT	58	9.67	89	40 (45%)	37 (42%)	12 (13%)
JD5_LPS	TILT	47	7.83	20	2 (10%)	15 (75%)	3 (15%)
JD5_FIXED	FIXED	60	10.00	52	7 (14%)	29 (56%)	16 (30%)
JD6	TILT/FIXED	125	20.84	319	76 (24%)	161 (50%)	82 (26%)

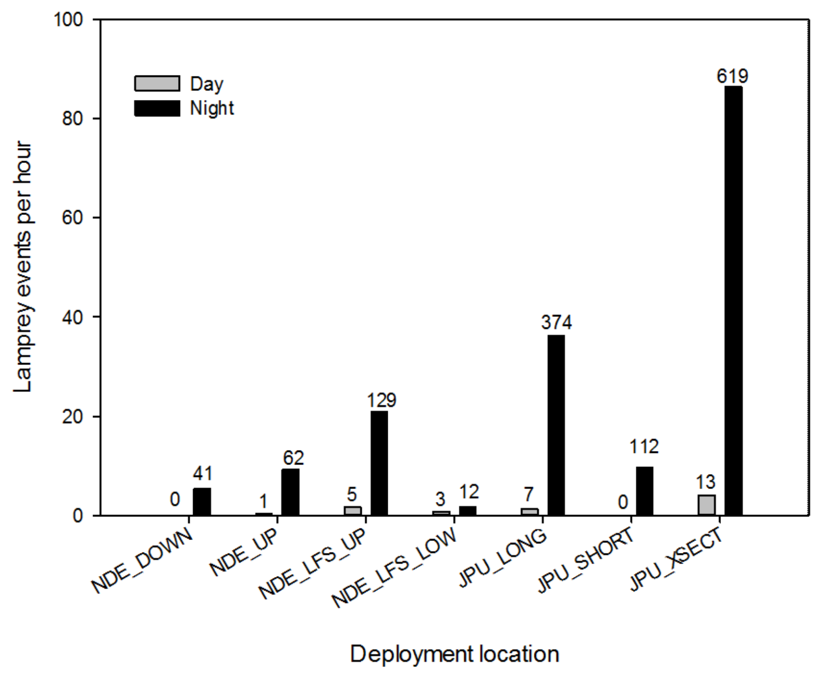

Figure 8. Number of lamprey events per hour during daytime and nighttime files at each of the seven deployment locations at Bonneville Dam. Note: TILT and FIXED data from JPU_SHORT and JPU_LONG were combined. Numbers of events are above each bar.

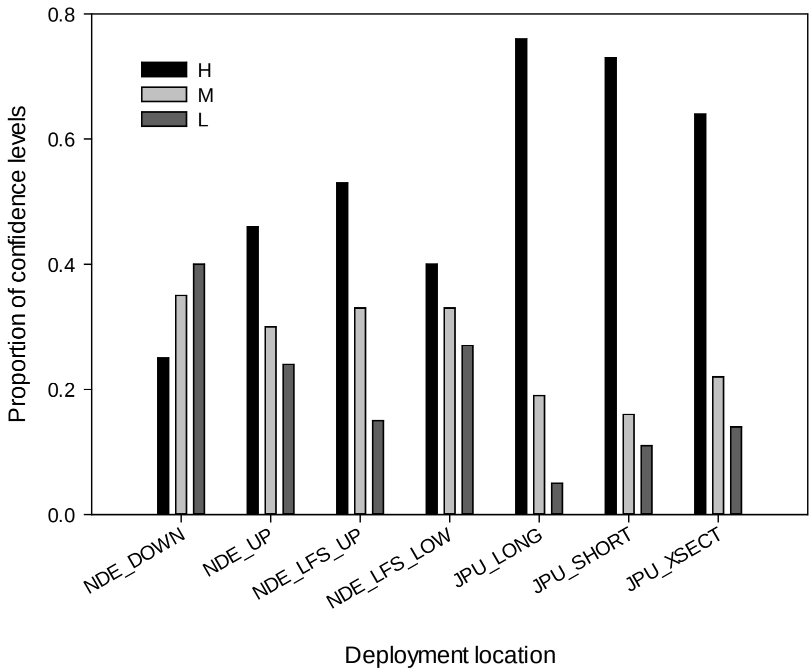

Figure 9. Proportion of events at each of the seven deployment locations for events that were classified as either high (H), medium (M), or low (L) confidence at Bonneville Dam. Proportions include both daytime and nighttime events. Number of events are provided in Table 3.

Bonneville Dam: Vertical distributions

At the JPU site, event rates varied considerably across the three deployment locations. Higher event rates were observed at JPU_XSECT (86.3/h) than at JPU_LONG (36.2 /h) and JPU_SHORT (9.7/h) (Figure 8). Lamprey were also distributed throughout the water column differently at these three locations. Event rates were higher in the upper sample volume along the south fishway wall (144.0/h) compared with the lower sample volume at the submerged overflow weir (20.2/h) at JPU_LONG. Event rates were also higher in the upper sample volume (44.2/h vs. 3.2 /h) at JPU_SHORT, where the upper sample deployment was oriented to capture the overflow weir whereas the lower sample deployment was oriented at the orifice. However, event rates were opposite at JPU_XSECT with higher event rates observed in the lower sample volume below the first submerged weir (121.3/h vs. 36.2/h) (Figure 10).

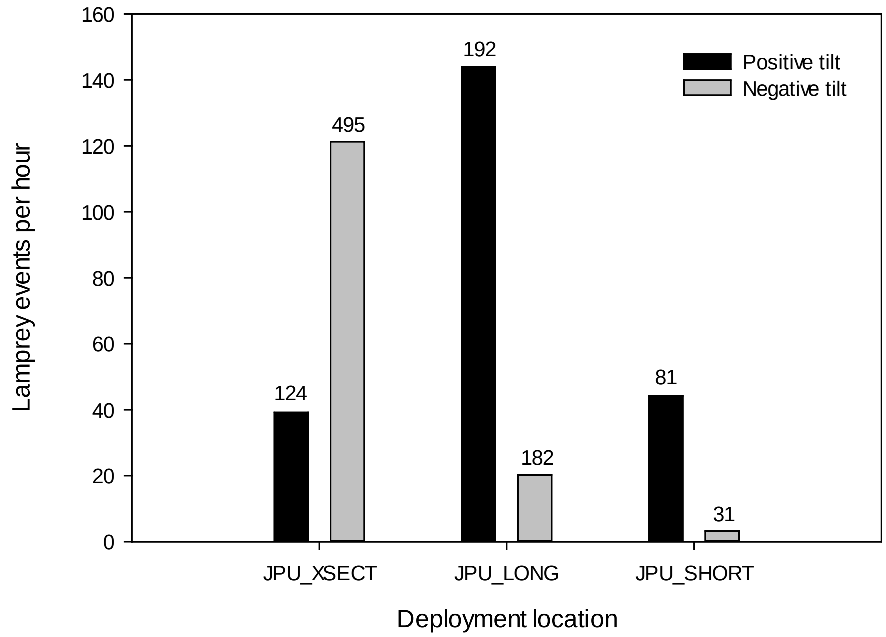

Figure 10. Number of lamprey events per hour at night in the lower sample volume (negative tilt) and upper sample (positive tilt) at the three JPU deployment locations at Bonneville Dam. Note: FIXED and TILT data from JPU_SHORT and JPU_LONG were combined. Numbers of events are above each bar.

Bonneville Dam: Fish orientation and upstream-downstream movements

The majority of lamprey events at NDE involved fish orienting upstream (i.e., into the prevailing flow). The highest proportion of upstream orientations was at NDE_ LFS_UP and NDE_UP (0.86), while the lowest proportion was at NDE_DOWN (0.75) (Table 4). Interestingly, the proportion of fish oriented upstream had declined by approximately one third from the time fish were first observed (0.72) compared with the time fish were last observed (0.42) by reviewers at NDE_UP (Figure 11). This change in orientation indicates that many fish turned around during the time they were observed.

Most lamprey moved upstream during the events observed at the NDE deployments. The proportion of upstream movements was higher at all NDE deployments (range: 0.68-0.75 upstream) than the proportion of downstream movements (Table 4). The orientation and movement directions of fish did not differ considerably between deployment locations at NDE, suggesting fish orienting upstream made overall net upstream progress. Net upstream movement, defined as the difference in the proportions of upstream and downstream movements, was greater than zero at all NDE deployments (range: +0.36 to +0.50).

Table 4. The proportions of both the orientation and upstream-downstream movement of lamprey at the four deployments at NDE, as well as the three JPU deployments in both the lower (negative tilt) and upper (positive tilt) sample volumes. Note: FIXED and TILT data from JPU_SHORT and JPU_LONG were combined. JPU proportions that do not sum to one are excluding "unknown" orientations.

Site	Tilt	Deployment	Orientation		Movement direction	
			Upstream	Downstream	Upstream	Downstream
NDE	None					
		NDE_DOWN	0.75	0.25	0.68	0.32
		NDE_LFS_UP	0.86	0.14	0.72	0.28
		NDE_LFS_LOW	0.80	0.20	0.75	0.25
		NDE_UP	0.86	0.14	0.75	0.25
JPU	Negative	JPU_LONG	0.29	0.20	0.49	0.51
		JPU_SHORT	0.22	0.19	0.42	0.58
		JPU_XSECT	0.27	0.40	0.47	0.53
	Positive	JPU_LONG	0.64	0.33	0.68	0.32
		JPU_SHORT	0.61	0.27	0.55	0.45
		JPU_XSECT	0.41	0.42	0.52	0.48

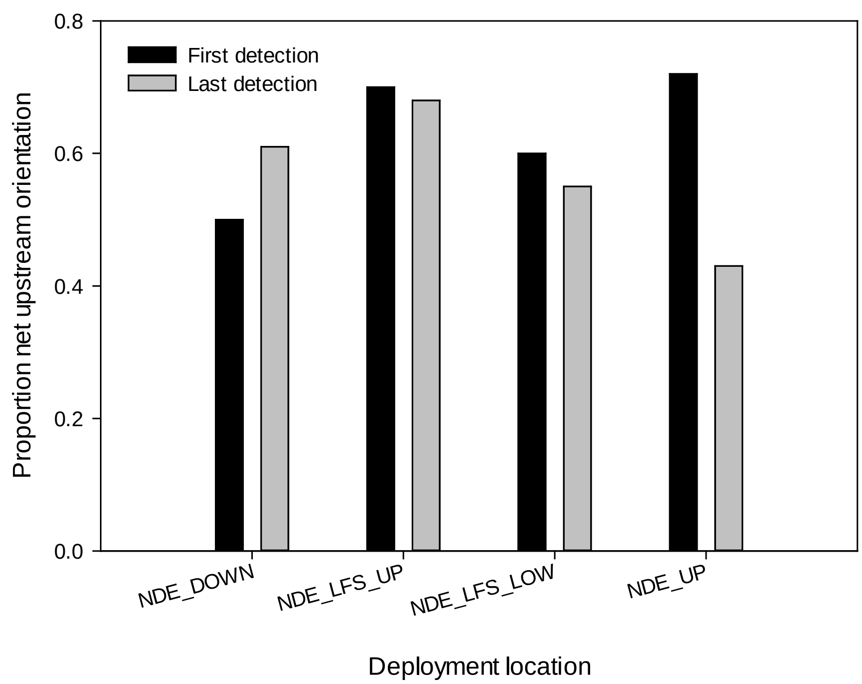

Figure 11. Net upstream orientation for the NDE deployment locations at Bonneville Dam. Bars are the proportion of fish oriented upstream when first detected by reviewers (black) and the proportion of fish oriented upstream when last detected by reviewers (gray).

The orientations of fish in the transition area varied both by the deployment location and position in the water column. In the upper sample volume, fish primarily oriented upstream or downstream, while orientations that were classified as “unknown” (i.e. indicating neither upstream nor downstream) were more common in the lower sample volume. The proportion of upstream orientations in the upper sample volume was highest at JPU_LONG (0.64) and lowest at JPU_XSECT (0.41). The proportion of downstream orientations in the upper sample volume was highest at JPU_XSECT (0.42) and lowest at JPU_SHORT (0.27). In contrast, the proportion of upstream (range: 0.22-0.29) and downstream (range: 0.19-0.40) orientations in the lower sample volume were low (Figure 12) because fish orientation was most commonly described as unknown (range: 0.32-0.58). Although they were classified as unknown, many of these movements were across the fishway channel (i.e., lateral), which was not one of the original event scoring classes.

Upstream-downstream movement patterns were similar to fish orientations in the upper sample volume. Upstream movement proportions were similar to fish orientation proportions at JPU_LONG (0.68 vs. 0.64, respectively) and JPU_SHORT (0.55 vs. 0.61, respectively), while the rate of upstream and downstream movements was relatively equal at JPU_XSECT (Table 4). Net upstream movements in the upper sample volumes were lower at JPU compared with NDE. JPU_SHORT (+0.34) had the highest proportions of net upstream movements, while there was little net upstream movement at JPU_SHORT (+0.10) and JPU_XSECT (0.04). In the lower sample volumes, the proportion of upstream movements (range: 0.42-0.49) was less than 0.50 and considerably less than in the upper sample volumes (Figure 13). Net upstream movements were negative at JPU_LONG (-0.02), JPU_XSECT (-0.06), and JPU_SHORT (-0.16).

Figure 12. Proportion of fish orientations in the upper (A) and lower (B) sample volumes at the three JPU deployment locations at Bonneville Dam based upon the swimming orientation of fish (Unknown, Downstream, and Upstream). Note: FIXED and TILT data from JPU_SHORT and JPU_LONG were combined.

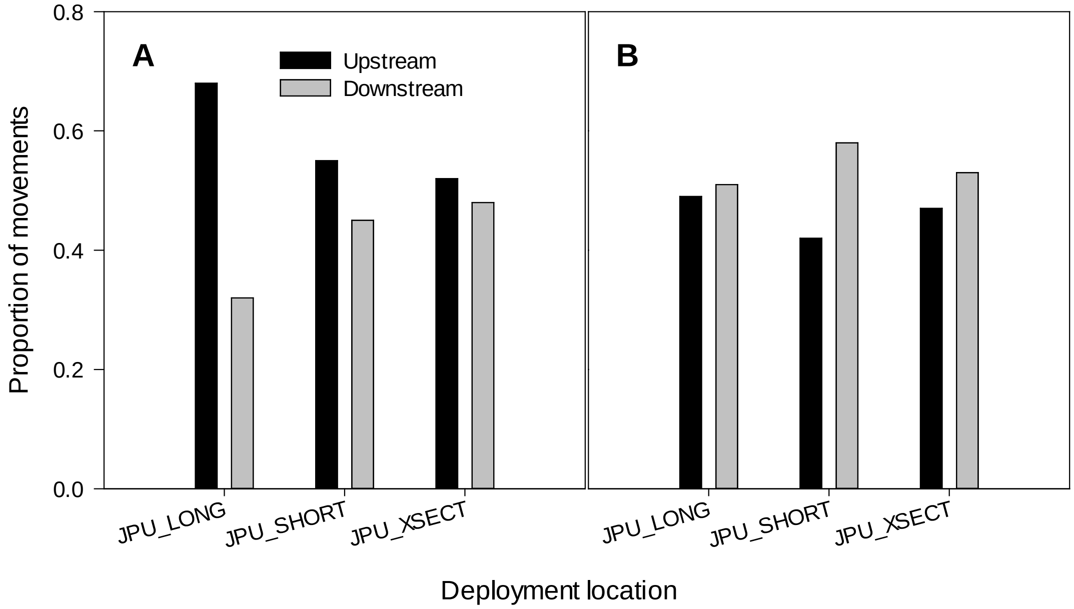

Figure 13. Proportion of fish movements (upstream or downstream) in the upper (A) and lower (B) sample volumes at the three JPU deployment locations at Bonneville Dam. Note: FIXED and TILT data from JPU_SHORT and JPU_LONG were combined.

Bonneville Dam: White sturgeon associations with lamprey

The distribution of lamprey and white sturgeon within the water column suggested that a potential negative correlation exists between lamprey event rate and sturgeon activity (Figure 15). Sturgeon presence was uncommon at the NDE deployment locations. The only observations of sturgeon were at the NDE_LFS_LOW deployment (2.1 hourly index score). Sturgeon activity indices were much higher at JPU, primarily in the lower sample volumes where the highest hourly index score ranged from 41.6 (JPU_SHORT) to 81.5 (JPU_LONG). Sturgeon indices were much lower in the upper sample volumes at JPU, with the highest rate at JPU_SHORT (28.8) (Figure 14; contrast with lamprey event rates in Figure 10).

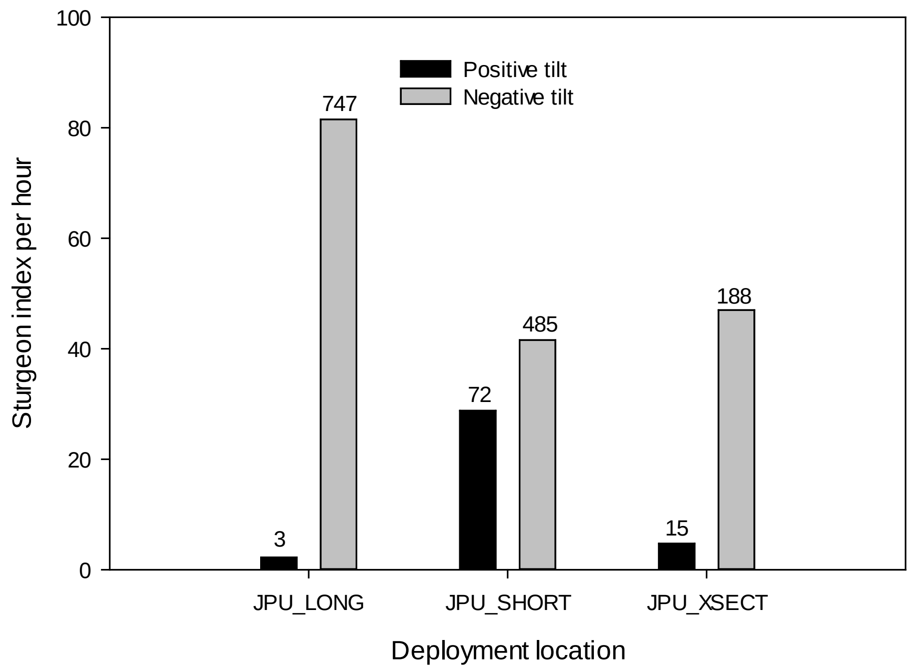

Figure 14. White sturgeon index of activity per hour for the upper (positive tilt) and lower (negative tilt) sample volumes at each JPU deployment location at Bonneville Dam. Numbers of observed sturgeon events per hour are above each bar. Note: FIXED and TILT data from JPU_SHORT and JPU_LONG were combined.

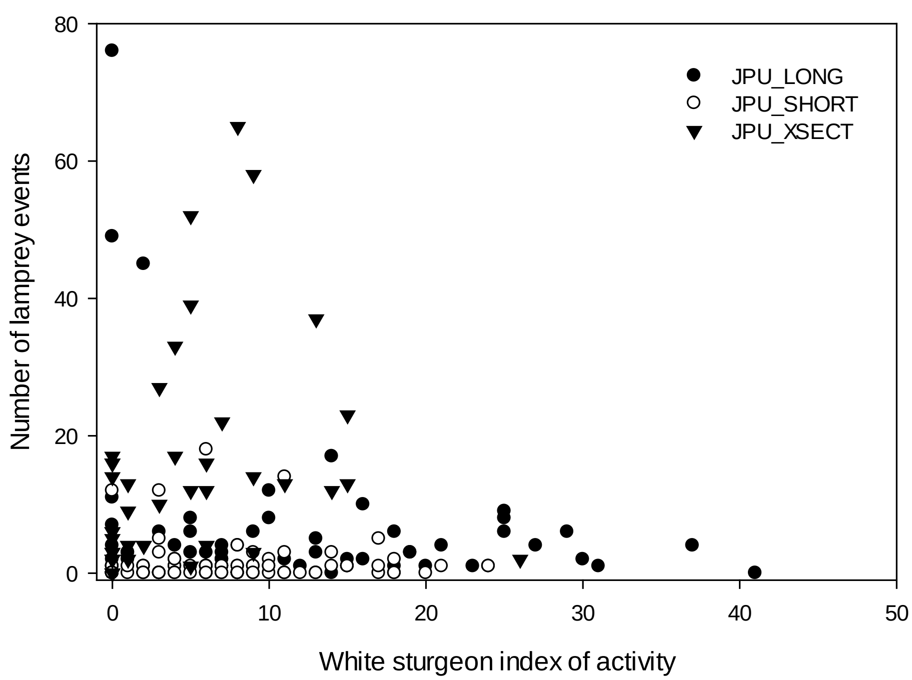

Figure 15. Number of lamprey events and an index of white sturgeon activity at the three JPU deployments at Bonneville Dam. Each point represents a ten minute file by deployment location. Note: FIXED and TILT data from JPU_SHORT and JPU_LONG are both included.

Bonneville Dam: Lateral distribution estimates

We used the mean range (distance from the camera) of individual lamprey events to estimate the lateral distribution (distance across the fishway) of lamprey at the transition area. The only deployment that spanned a wide range of the fishway channel and captured the opposite wall was the upper sample volume at the JPU_LONG deployment. The proportion of upstream lamprey movements occurred evenly across the lateral plane in the unweighted estimates (n = 124, range: 0.02-0.16), with the highest proportion occurring in the 3.5-4 m range bin. In contrast, the proportion of downstream movements (n = 64, range: 0.04-0.40) in the farthest range bin near the wall was twice as high as any other proportion in the lateral plane (Figure 16).

In the weighted estimates, the proportions of both upstream and downstream events were higher in range bins closer to the camera. For upstream events, the highest proportion of events was observed in the 2.5-3 m range bin and there was greater variability in the proportion of events across the lateral plane (range: 0.02-0.31) with fewer events in the most distant range bins. For downstream events, the highest proportion of events was still observed in the farthest range bin near the wall and the events were distributed slightly more evenly (range: 0.03-0.21) (Figure 16) across the lateral plane compared to unweighted estimates.

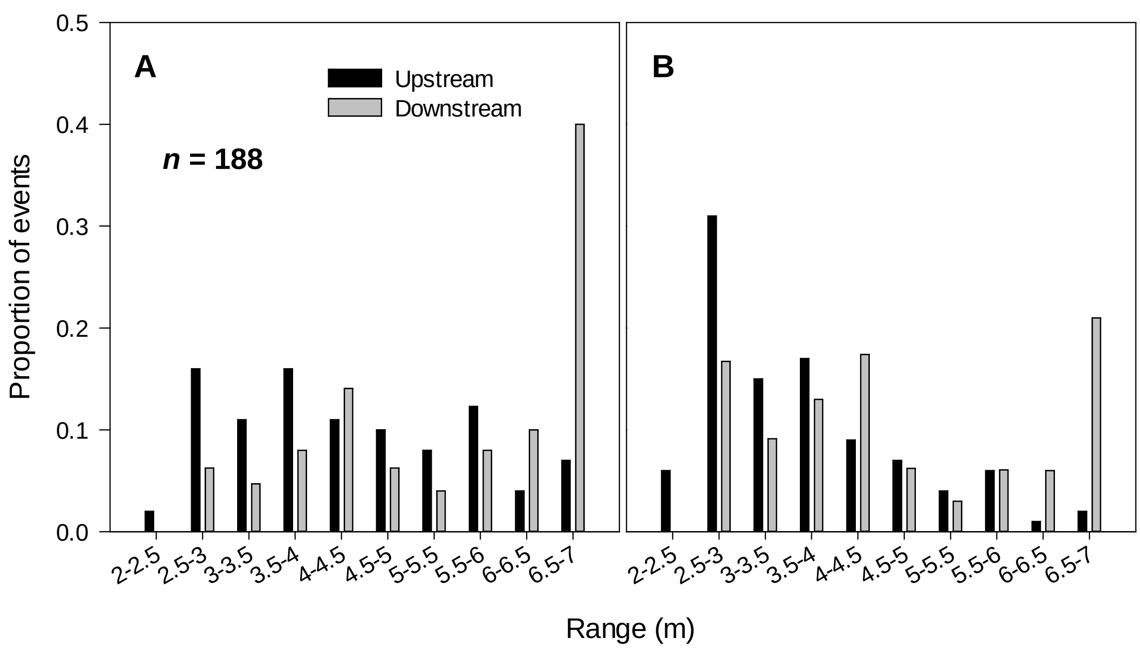

Figure 16. Unweighted (A) and weighted (B) estimates of the lateral distribution of lamprey movements (upstream, downstream) in the upper sample volume at the JPU_LONG deployment at Bonneville Dam. Weighted estimates were included to account for differences in the DIDSON's sample volume. The farthest range bin captured the south fishway wall.

Bonneville Dam: Late season deployment comparisons

There were very few events in the late season deployments at JPU_SHORT (*n* = 4). Event rates were higher for early versus late season deployments at both the overflow weir in the upper sample volume (44.2 vs. 3.2, respectively) and at the orifice in the lower sample volume (3 vs. 1, respectively). Regarding the JPU_XSECT_LATE deployment, we observed 36 lamprey events in 27 nighttime files (4.5 h) for an event rate of 8.0 events per hour, which is considerably lower than the early season JPU deployments. The largest proportion of these events were classified as high confidence (0.53) with similar proportions for medium (0.22) and low (0.25) confidence events. The proportion of fish orienting upstream at this deployment (0.71) was slightly higher than at earlier JPU deployments. See Appendix A and B for more details regarding this deployment.

Table 5. Summary of the number of events, files, and events per hour for the early and late season deployments made at the JPU_SHORT location at Bonneville Dam. Deployments using a positive tilt oriented towards the overflow weir and deployments using a negative tilt oriented at the orifice of the second overflow weir in the transition area.

Deployment site	Time/Season	Tailrace elevation (m)	Tilt	Events	Files	Events per hour
JPU_SHORT	Early	4.7-6.6	Positive	81	11	44.18
			Negative	31	58	3.21
	Late	3.7	Positive	2	4	3.00
			Negative	2	12	1.00

Bonneville Dam: Water velocity and lamprey ground speed estimates

We estimated the swim speeds for 109 individual lamprey from 29 files across six deployments. Only nighttime files were evaluated. The JPU deployments (*n* = 79) had more estimates than the NDE deployments (*n* = 30) due to the lower number of events observed at NDE. Estimated mean water velocities were higher for the combined NDE deployments (0.87 m/s) than the combined JPU deployments (0.32 m/s). The highest water velocities were observed at NDE_UP (mean = 1.16 m/s) and the lowest were at JPU_SHORT (mean = 0.24 m/s). Water velocities differed considerably between the three NDE deployments (range: 0.46-1.16 m/s), while estimates at JPU were relatively similar for all three deployments (range: 0.24-0.43 m/s) (Figure 17).

Although water velocity estimates differed between deployments, lamprey ground speed estimates did not differ between JPU (mean = 0.78 m/s, *n* = 79) and NDE (mean = 0.79 m/s, *n* = 30). Ground speeds were highest at NDE_LFS_UP (mean = 0.89, *n* = 9) and lowest at NDE_DOWN (mean = 0.64 m/s, *n* = 6) (Figure 17). Swim speeds through water for lamprey were thus higher at NDE (mean = 1.60 m/s) than at JPU (mean = 1.09 m/s) given the higher estimates of water velocity. Lamprey swim speed estimates through water were highest at NDE_UP (mean = 1.96 m/s, *n* = 15), were lower at NDE_LFS_UP (mean = 1.36 m/s, *n* = 9) and NDE_DOWN (mean = 1.40 m/s, *n* = 6), and were lowest at the three JPU deployments (range: 0.99-1.12 m/s) (Figure 17).

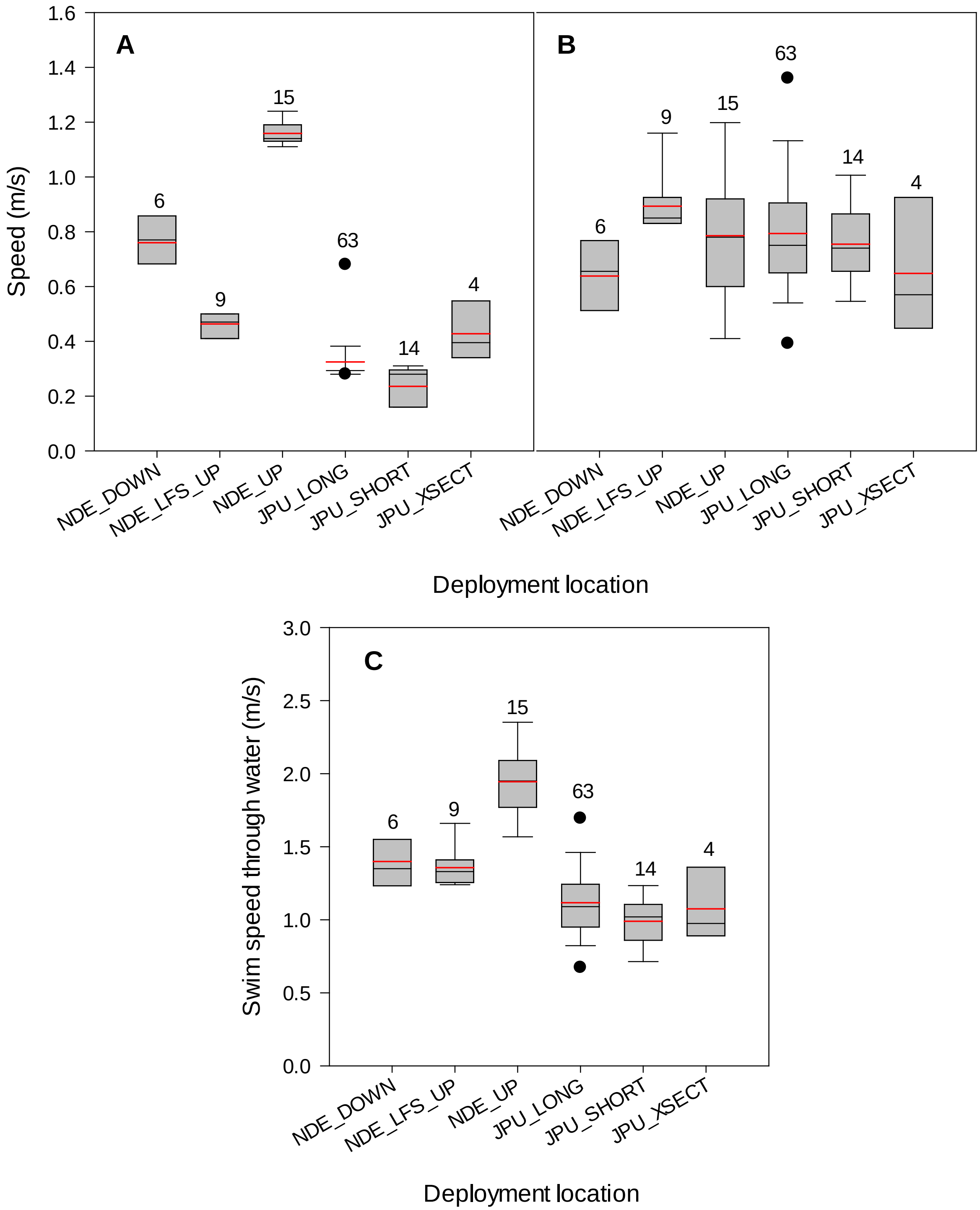

Figure 17. Estimates of (A) water velocity, (B) ground speed for individual lamprey , and (C) swim speeds through water for individual lamprey at the six deployment locations at Bonneville Dam. Box plots show 5th, 10th, 25th, 50th, 75th, 90th, and 95th percentile estimates. Red lines are mean values. Numbers above each box are the number of fish for each location.

Bonneville Dam: Tail-beat frequency estimates

We estimated the tail-beat frequencies (TBF) for a total of 82 fish from five deployments. There were fewer estimates from NDE (n = 11) than JPU (n = 61). The mean TBF was higher for the combined NDE deployments (3.54 beats/sec) than the combined JPU deployments (2.82 b/s). The highest mean TBF estimate was at NDE_UP (4.03 b/s, n = 8), while NDE_LFS_UP (2.22 b/s, n = 3) had the lowest estimate. JPU had relatively similar TBF estimates across the three deployments (range: 2.44-2.87) (Figure 18). For 73 fish that had both ground speed and TBF estimates, we found a positive correlation between lamprey swim speeds through water and TBF (r = 0.61, p < 0.01) (Figure 19). Weaker correlations were observed with both ground speed (r = 0.40, p < 0.01) and water velocity (r = 0.42, p < 0.01), but swim speeds through water provided the strongest correlation since it accounted for the variation of both. Notably, there was considerable unexplained variation in the relationship between TBF and swim speed through the water.

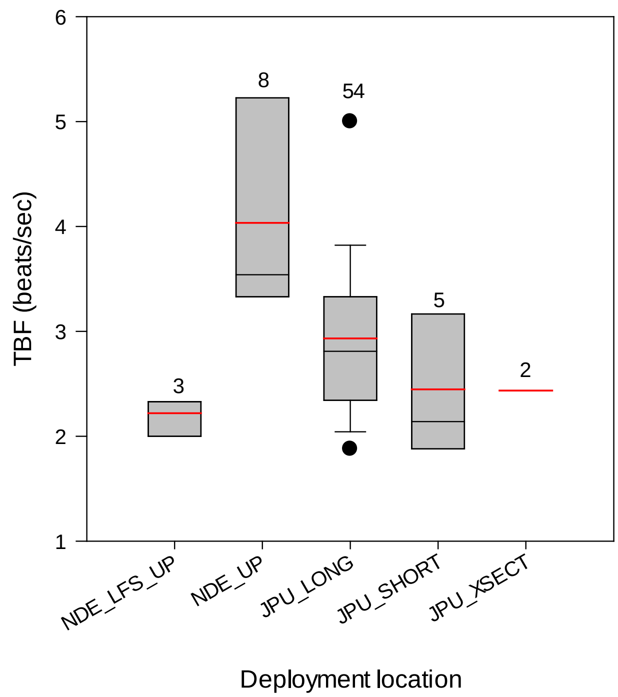

Figure 18. Tail-beat frequencies for individual lamprey at five deployment locations at Bonneville Dam. Box plots show 5th, 10th, 25th, 50th, 75th, 90th, and 95th percentile estimates. Red lines are mean values. Numbers above each box are the number of fish for each location

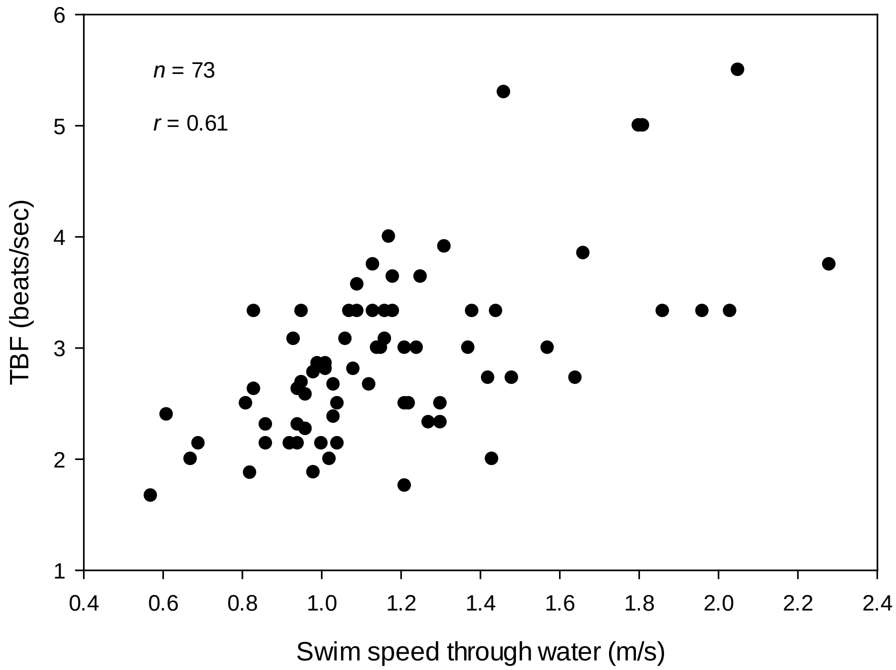

Figure 19. Plot displaying the positive correlation between lamprey swim speed through water and TBF for 73 fish from the five deployment locations at Bonneville Dam (Figure 18).

John Day Dam

John Day Dam: Event rates and confidence levels

At the seven deployments in the John Day north fish ladder, we observed a total of 614 lamprey events with most near the fishway entrance at JD6 (*n* = 319, Table 3). A total of 74 events were observed during the day, mostly at JD6 (*n* = 27), which also had the highest daytime event rate (5.8 events per hour; Figure 20). Nighttime event rates varied considerably across sites. The highest nighttime rate was at JD6 (21.5 events/h) and the lowest was 0.5 events/h in the transition area at JD4.

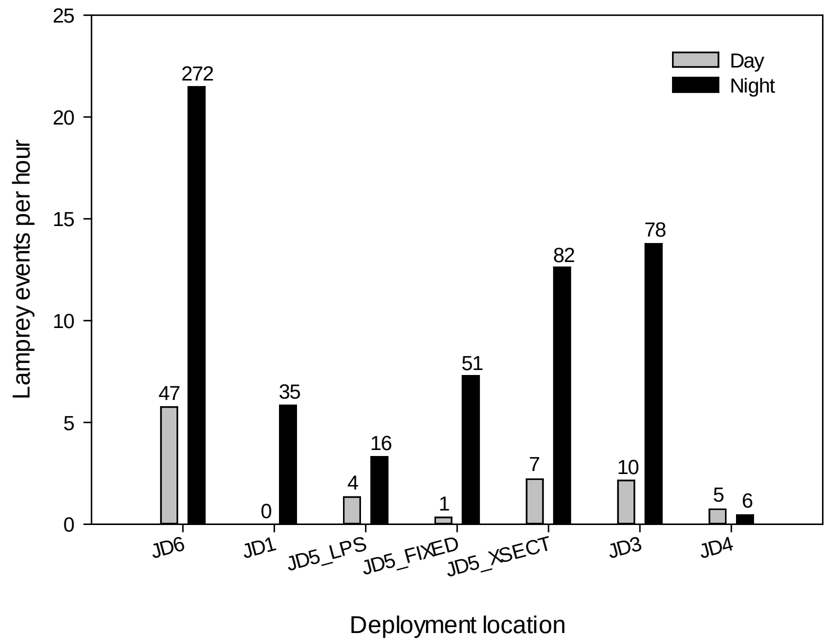

Figure 20. Number of lamprey events per hour during daytime and nighttime files at each of the seven John Day deployment sites. Deployment locations are listed in order of proximity to the fishway entrance (J6 = closest, JD4 = farthest). Note: FIXED and TILT data from JD6 were combined. Number of events are above each bar.

Similar to Bonneville, confidence levels varied across the different deployments (Figure 21). The highest proportion of high confidence events was at JD3 (0.68), while no events were classified with high confidence at JD5_LPS. The highest proportion of low confidence events was at JD4 (0.50), although the number of observations was relatively small (n = 11). Cross-sectional deployments (JD1, JD3, JD5_XSECT) had higher proportions of high confidence events (range: 0.47-0.68) than bollard field deployments (JD6, JD5_FIXED) (range: 0.13-0.22). Similar to Bonneville, we excluded all daytime events and files from the remaining analyses given the limited conclusions we could draw from them.

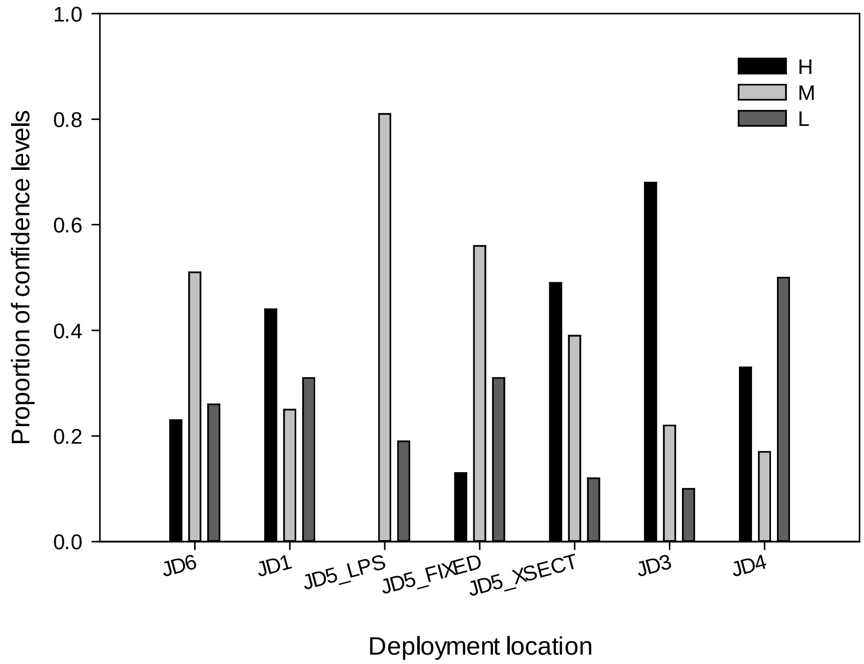

Figure 21. Proportions of events at each of the seven John Day deployments for events that were classified as either high (H), medium (M), or low (L) confidence. These include both daytime and nighttime events. Locations are ordered based on their distance from the fishway entrance. Number of events are in Table 3.

John Day Dam: Attachment behaviors

We observed a total of 245 attachment events across the seven different deployments. Four events (2%) were observed at JD5_XSECT, 46 (19%) were at JD5_FIXED, and 189 (77%) were at JD6. All of the attachments at the fishway entrance area occurred in the bollard field. We also observed 6 six attachments upstream in the collection channel at JD3 where fish were observed attaching to the fishway floor.

John Day Dam: Vertical distributions

Lamprey events were higher in the lower sample volumes for all six tilt deployments at John Day Dam (Figure 22). The highest event rates observed in the lower sample volume were at JD6 (28.5/h) and JD3 (27/h). The highest event rate in the upper sample was at JD5_XSECT, where event rates were similar between the upper and lower sample volumes (12.0/h vs. 13.2 /h, respectively). No fish were observed in the upper sample volume at JD5_LPS. Lamprey presence was low in both the upper and lower sample volumes at JD4 in the transition area (0.2 and 0.4/h, respectively).

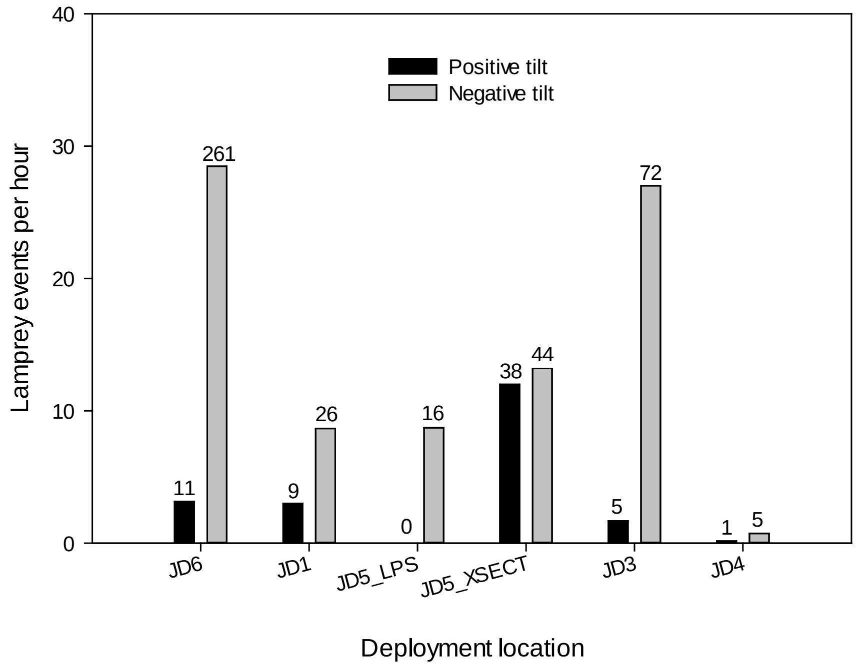

Figure 22. Lamprey events per hour at the six tilting deployments in the John Day Dam fishway. Gray bars indicate event rate during negative tilt (lower sample volume) and black bars indicate event rate during positive tilting (upper sample volumes). Note: FIXED and TILT data from JD6 were combined. Number of events are above each bar.

John Day Dam: Fish orientation and upstream-downstream movements

The upstream and downstream orientation of lamprey varied among deployments and depth strata. The majority of lamprey were observed orienting upstream regardless of camera tilt angle (Table 6). The highest proportion of fish orienting upstream was in the lower sample volume at JD3 (0.97) and the lowest was at JD5_LPS (0.69). (Excluding JD4, where n = 6 total events). Proportions of lamprey orienting upstream in the upper sample volumes (range: 0.56-0.84) were typically less than proportions in the lower sample volumes (range: 0.69-0.97). No lamprey were observed in the upper sample volume at JD5_LPS. No lamprey were classified with an unknown orientation in the observations at John Day Dam.

The proportion of fish moving upstream was higher in the lower sample volumes (range: 0.56-0.92) than the upper sample volumes (range: 0.22-0.58) (Figure 23). The proportion of upstream movements and proportion of fish observed orienting upstream differed considerably for most deployments, although greater differences were observed in the upper sample volumes (Table 6). The highest net upstream movements were observed at JD3 (+0.84) and JD5_XSECT (+0.82) in the lower sample volume. Net upstream movements were lower in the upper sample volume where no net upstream movement was observed at JD3 (0) and a negative net upstream movement was observed at JD1 (-0.56).

Table 6. The proportions of both orientation and upstream-downstream movement of fish at the five tilt deployments at John Day Dam in both the lower (negative tilt) and upper (positive tilt) sample volumes.

Tilt	Site	Orientation		Movement direction	
		Upstream	Downstream	Upstream	Downstream
Negative	JD1	0.74	0.26	0.56	0.44
	JD3	0.97	0.03	0.92	0.08
	JD4	0.60	0.40	0.60	0.40
	JD5_XSECT	0.91	0.09	0.91	0.09
	JD5_LPS	0.69	0.31	0.58	0.42
Positive	JD1	0.56	0.44	0.22	0.78
	JD3	0.67	0.33	0.50	0.50
	JD4	1.00	0	1.00	0
	JD5_XSECT	0.84	0.16	0.58	0.42
	JD5_LPS	0	0	0	0

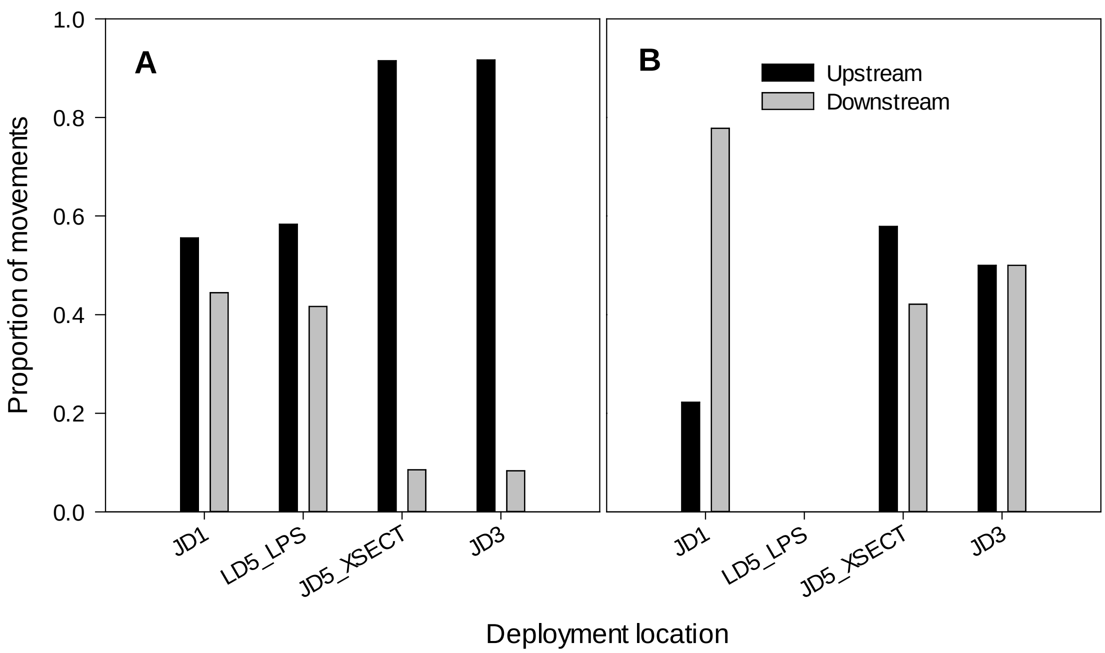

Figure 23. Proportion of upstream-downstream movements in the lower (A) and upper (B) sample volumes at four tilt deployments at John Day Dam. Note: JD6 is not included because the lower sample volume included the bollard field and the orientation of fish was difficult to identify. JD4 was not included given the few number of events ($n = 6$). Additionally, no events were observed in the upper sample volume at JD5_LPS.

John Day Dam: White sturgeon associations with lamprey

Indices of sturgeon activity varied across the six John Day tilt deployments, although there was consistently higher activity in the lower sample volumes versus the upper sample volumes. The highest hourly index score for the lower sample volumes was observed at JD4 (9.7) and the lowest was at JD3 (0.4) (Figure 24). The range of sturgeon activity was much lower in the upper sample volumes (range: 0-0.8). Unlike at Bonneville Dam, both lamprey and sturgeon were more often observed in the lower sample volumes at all John Day locations (compare with Figure 22). Nonetheless, a negative correlation may exist between lamprey event rate and sturgeon activity, especially at the JD4 location in the transition area (Figure 25).

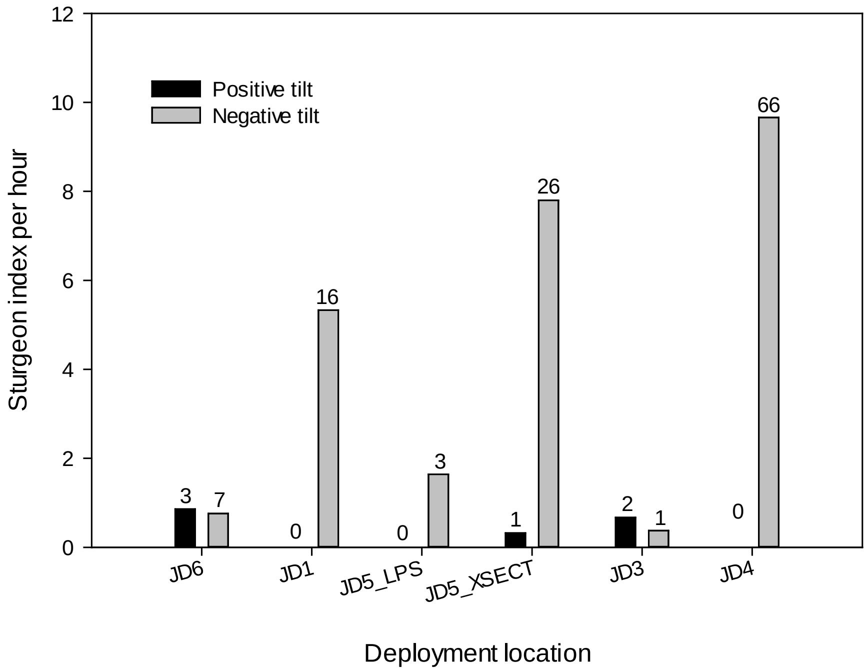

Figure 24. White sturgeon index of activity per hour for the upper (positive tilt) and lower (negative tilt) sample volumes at the six TILT deployments at John Day Dam. Note: FIXED and TILT data from JD6 were combined. Number of events are above each bar.

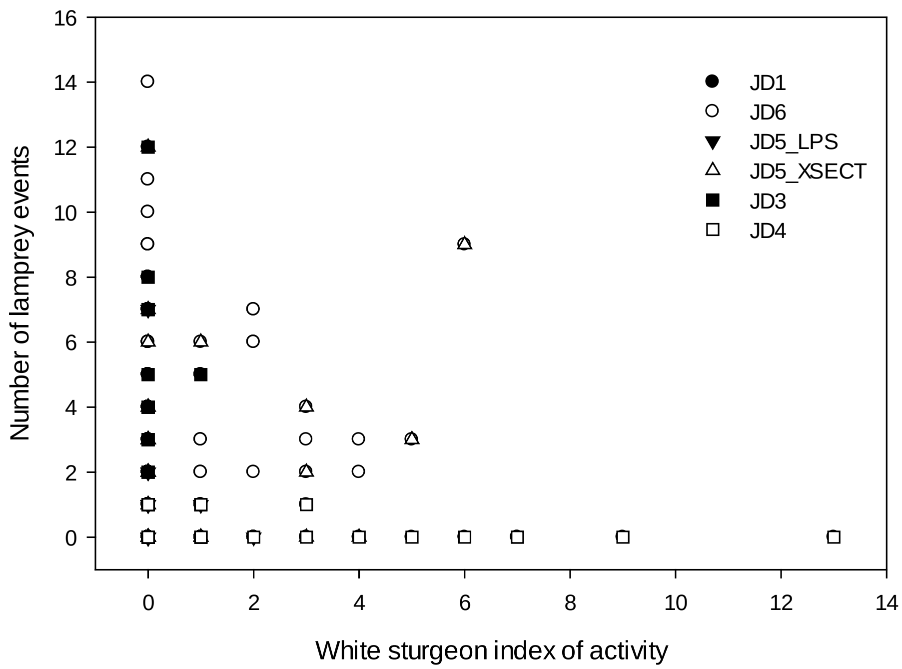

Figure 25. Plot displaying the relationship between number of lamprey events and white sturgeon activity at the six tilt deployments at Bonneville Dam. Each point represents a ten minute file, which are sorted by deployment location.

John Day Dam: Lateral distribution estimates

At John Day, we estimated the lateral distribution of lamprey at the JD5_XSECT and JD5_LPS deployments. At JD5_XSECT, the unweighted proportion of upstream events in the upper sample volume was highest primarily in the farthest range bins (n = 20, range: 0.05-0.5), with the proportion in the farthest range bin over twice as high as any other estimate. The proportion of downstream movements were also higher in the farthest range bins in the upper sample volume (n = 16, range: 0.05-0.32) (Figure 26). In the lower sample volume, the proportion of upstream events was three times higher in the farthest range bin than in any other bin (n = 41, range = 0.02-0.32). The proportion of downstream events in the lower sample volume on the other hand was greater in the range bins closer to the camera, although there were only three events (Figure 26).

Similar to Bonneville, weighted estimates increased the proportion of both upstream and downstream events closer to the camera. In the upper sample volume, the highest proportion of upstream events was still observed in the farthest range bin (range: 0.05-0.36). For downstream events, the range of events remained highest in the farthest range bins as well (Figure 26). In the lower sample volume, weighted estimates suggested that there was a more even distribution of upstream events across the fishway floor (range: 0.05-0.22) compared with the unweighted estimates.

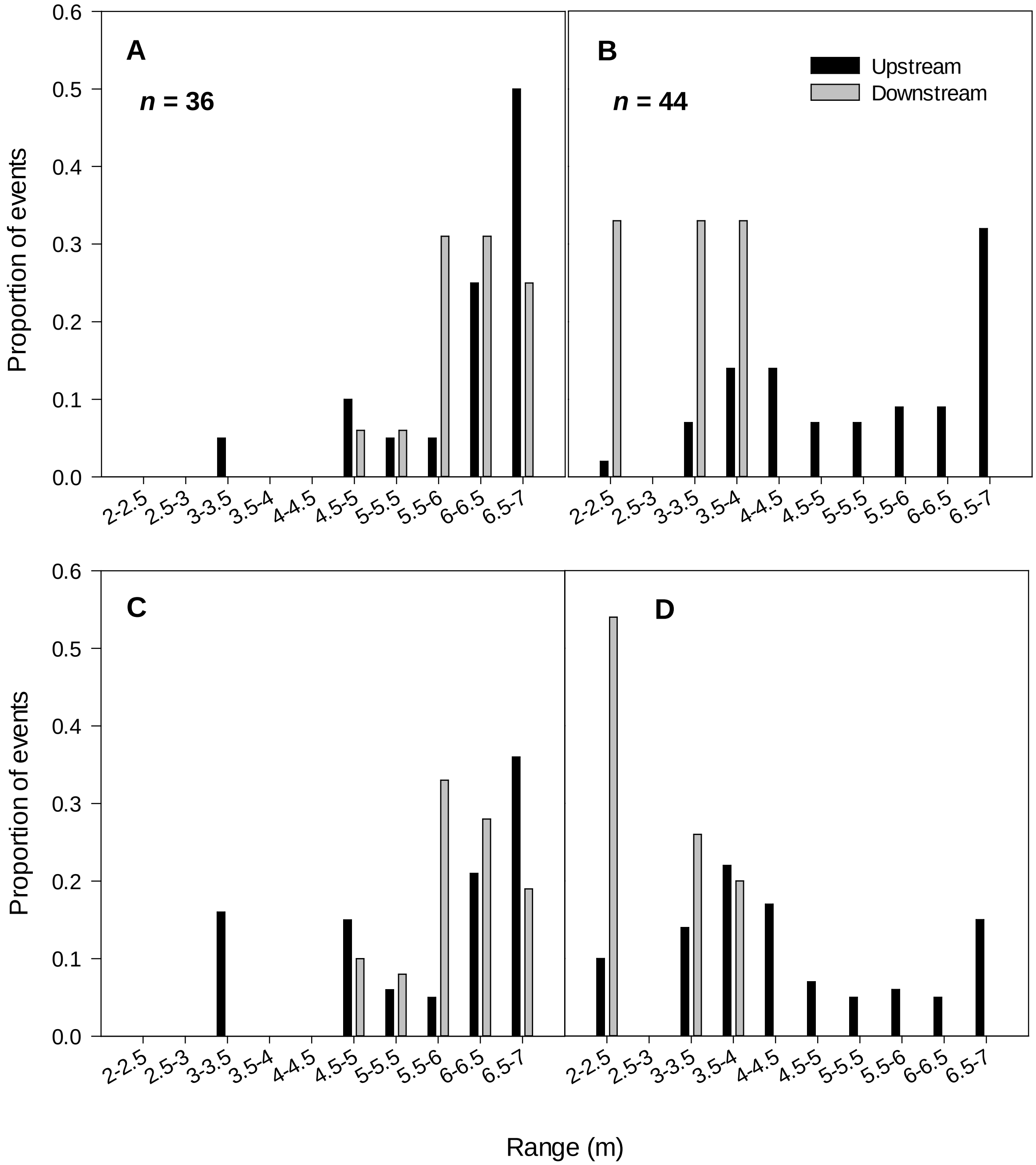

Figure 26. Unweighted estimates on the lateral distribution of lamprey movements (upstream, downstream) in the (A) upper and (B) lower sample volume at the JD5_XSECT deployment at John Day Dam. Weighted estimates for the (C) upper and (D) lower sample volume account for differences in the DIDSON sample volume. Note: the JD5_XSECT deployment did not capture the north fishway wall in the furthest range bin and likely underestimates the full extent of lamprey distribution at this location.

Lateral distribution estimates were only made in the lower sample volume for JD5_LPS since no events were observed in the upper sample volume. In the unweighted estimates based on small sample sizes, all of the upstream events (*n* = 11, range: 0.14-0.43) were in the farthest range bins with the highest proportion of upstream events in the 6.5-7.0 m range bin. Downstream events were also highest in the farthest range bins, but the sample was small (*n*=5). Weighted estimates showed a relatively similar distribution (Figure 27).

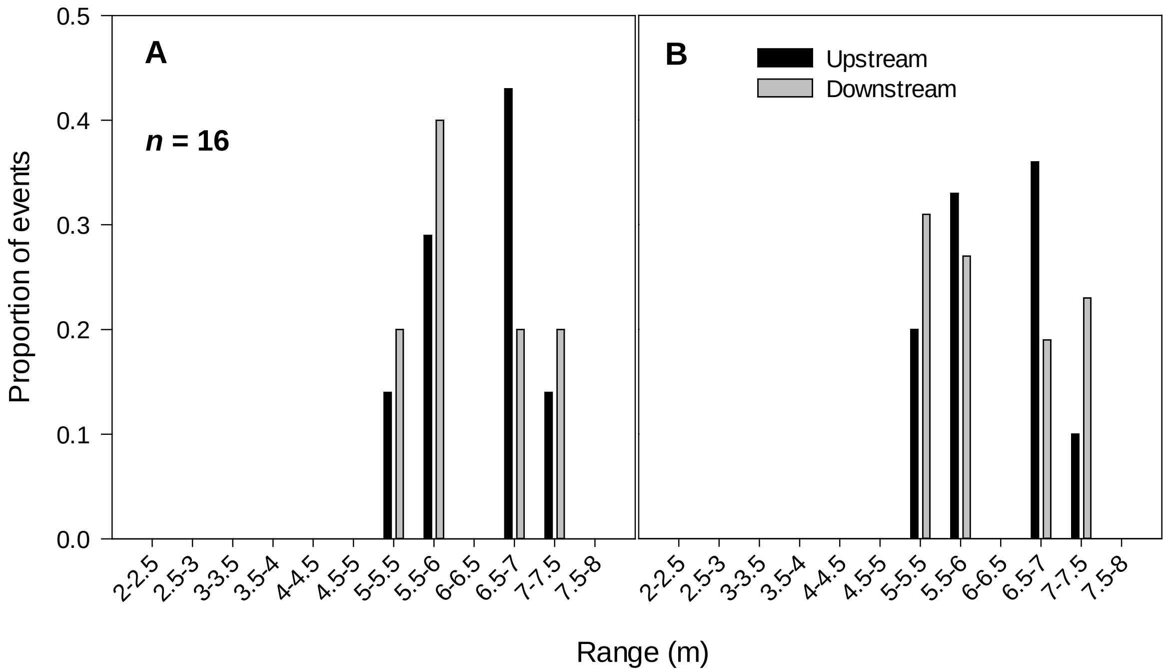

Figure 27. Unweighted (A) and weighted (B) estimates on the lateral distribution of lamprey movements (upstream, downstream) in the lower sample volume at the JD5_LPS deployment at John Day Dam. No events were observed in the upper sample volume. Weighted estimates are used to account for differences in the DIDSON sample volume. The range at 8 meters captured the lamprey passage structure (LPS) and north fishway wall.

Discussion

Among-viewer comparisons and confidence level classifications

As in previous studies, we compared lamprey events across a set of identical multi-viewer files as a measure of quality control. Our previous studies have suggested that inter-observer effects (i.e. viewer willingness to score an event, detection probability based upon duration time) result in scoring differences among viewers. While low detection probability and shorter event durations will likely underestimate lamprey activity, variation in the willingness to score events can bias estimates between reviewers (Johnson et al. 2013; *in review*). For these reasons, we have advocated the use of these quality control measures and the four identification criteria to help standardize lamprey identification and reduce potential differences among viewers.

Many of the differences in viewer agreement and confidence level classification that were observed across deployments resulted from site-specific factors at each location. The higher agreement between deployments in the Bonneville transition area was likely a result of the high quality imagery that was collected at these deployments. In contrast, high turbulence at NDE created interference in the imagery that may have hindered the reviewer's ability to distinguish lamprey from other species. A similar effect was observed within the bollard fields at John Day Dam where high turbulence and acoustic reflection generated within the bollard field resulted in more events being classified with lower confidence. Cross-sectional deployments that captured fish swimming perpendicular to the camera had higher proportions of high confidence events. Similar constraints have been documented for distinguishing fish species with DIDSON when there are differences in fish orientation (i.e. swimming parallel vs. perpendicular to the camera) or orientation of the camera (landscape vs. portrait) (Pipal et al. 2012; Johnson et al. *in review*).

2013 Sampling constraints

A number of important caveats need to be addressed regarding the sampling design for the 2013 DIDSON studies before considering the implications of the results. Some deployments at John Day Dam, as well as the NDE_UP and NDE_DOWN deployments at Bonneville Dam, occurred during only one overnight period and likely did not capture enough temporal variation in the behavior and abundance of lamprey at those locations (Appendix A provides the number of dates for each deployment). The limited sampling was due, in part, to turbulence-related damage that the DIDSON suffered at the NDE deployment. Similarly, the late season deployments at Bonneville Dam were necessarily qualitative given the limited sampling dates and viewing effort associated with generally poor image quality as a result of tailwater changes. There were also several inconsistencies between the 2012 and 2013 deployments at JD1 and JD3 where the south fishway wall was not captured in 2013, which limits the direct comparability of these results.

Lamprey event rates

Lamprey exhibited a clear diel pattern in their passage behaviors. Although daytime events did occur, event rates were much higher at night at both Bonneville and John Day dams. This was not surprising because it is well established that Pacific lamprey are primarily nocturnal during their upstream migrations (Moser et al. 2002b; Keefer et al. 2013a). Event rates at NDE were substantially lower in our 2013 studies (range: 5.35-10.93 events per hour) than in 2012 (range: 15.00-45.00), but this was likely a function of deployment effort and seasonal timing. Only one nighttime deployment was made for each of the NDE_UP and NDE_DOWN deployments, which may not have been representative of the abundance and behavior of fish approaching NDE. Another potential explanation is that the NDE deployment in 2012 was oriented across channel from the opposite (south) side of the channel, had better video quality, and thus may have allowed for easier lamprey identification. The camera was positioned in the line of flow in 2013, and the force from the outflow frequently produced interference and reduced video quality. Lastly, the daytime lamprey counts at Bonneville Dam were ~20% higher in 2012 (29,224) than in 2013 (23,970) (Columbia Basin Research 2014).

The highest event rates at NDE were observed in the NDE_LFS_UP deployment, which captured imagery surrounding the lamprey flume system (LFS) that was installed the previous spring. The LFS was operational during all three overnight deployments. Three fish were collected from the LFS during the 6/20-6/21 overnight period and no fish were collected during the other two overnight deployments (7/16-7/17 and 7/17-7/18). No lamprey were observed entering the LFS in the DIDSON imagery, although many fish were observed orienting upstream towards the LFS and several fish swam in close proximity to the entrance slot. The differences in event rate between the two LFS deployments may have been associated with temporal changes in abundances or behavior. Those differences may also have been a result of changes that the LFS underwent in late June-early July, which resulted in very few fish passing through the system for the remainder of the year.

Lamprey event rates were much higher in the Bonneville transition area than at NDE. Repeat observations of individual fish were likely since we observed such a large number of upstream and downstream movements in the upper sample volumes of the water column at the transition area, which is a known passage bottleneck with high turn-around rates for lamprey (Keefer et al. 2013c). Additionally, individual fish were probably observed multiple times in the lower sample volumes of the water column where many fish swam back and forth across the fishway channel. Because it is impossible to track and identify individual fish movements using DIDSON, some events observed within viewing files are possibly the same fish passing the DIDSON repeatedly (Boswell et al. 2008). This implies that there is a potential to overestimate the number of lamprey within the fishway, which is one constraint in using the DIDSON to calculate fish passage metrics (Johnson et al. *in review*). Nonetheless, such observations are valuable for identifying potential behavioral patterns (i.e. milling) at specific locations.

Lamprey event rates at John Day Dam were similar in 2012 and 2013 at JD1 and JD4, but rates were almost four times as high at JD3 in 2013. Additionally, event rates were also higher for several of the new JD5 and JD6 deployments compared to any 2012 deployment, which was likely a result of those deployments obtaining imagery closer to the fishway entrance and providing broader coverage of the bollard field. These between-year differences may also have been a result of lower sampling effort in 2013, similar to NDE at Bonneville Dam. During the only overnight deployment at the John Day LPS (7/22-23), no fish were collected from the LPS the following day and no fish were observed entering the system from DIDSON footage. Interestingly, one fish from the multi-viewer files (excluded from analyses) was observed attached to the outside wall of the LPS before proceeding upstream through the collection channel. Although the LPS deployment had the lowest event rate for all the lower collection channel deployments, many lamprey were observed orienting upstream near the LPS.

Excluding the JD3 deployment, the number of events generally decreased upstream through the collection channel and the number of events observed at the transition area was very low. Both of these patterns were similar to the 2012 results. The high attrition observed through the collection channel may be a result of high velocities through this region. Unlike at Bonneville Dam, no nighttime velocity reductions (e.g., Johnson et al. 2012a) were done to facilitate lamprey passage at John Day Dam. Although unreported here, water velocity estimates that have been calculated from our 2012 John Day DIDSON data suggests water velocities range from 1.5-1.8 m/s through the entire length of the collection channel (Kirk, *unpublished data*). Although these estimates are below the reported burst speed capabilities of Pacific lamprey (2-2.5 m/s, Keefer et al. 2010, 2011), the sustained high-velocity fields through the long collection channel could potentially exceed the endurance swimming capabilities of lamprey (Katopodis and Gervais 2012). There are other potential mechanisms for explaining the limited number of events observed at JD4 such as poor passage through the turn pool or the negative association with white sturgeon in the transition area.

Attachment behaviors

Unlike previous years, we observed no lamprey at Bonneville Dam engaging in attachment events using their oral discs. However, attachment events in past DIDSON studies at Bonneville were relatively infrequent and site dependent (i.e., they were occurred mostly at high-velocity sites). We initially hypothesized that lamprey would frequently engage in attach-and-burst events to propel themselves through areas of high velocity (Kemp et al. 2009). These behaviors had been observed under high-velocity conditions in an experimental flume (Keefer et al. 2010, 2011). Lack of attachment events was presumably a consequence of low water velocity and high sturgeon presence in the transition area, and perhaps reduced night-time velocity at the NDE site. In contrast, large numbers of attachment events by lamprey were observed at John Day Dam in both 2012 and 2013. Nearly all events were in the bollard field at the fishway entrance, although a few fish in 2013 were observed attaching to the fishway floor upstream in the collection channel, possibly in part because the floor of this segment is primarily composed of diffuser grating.

Several factors may explain why more attachments events were observed at John Day than at Bonneville Dam. First, velocities in fishways at Bonneville were reduced at night, but not at John Day Dam. The reduced nighttime flows at Bonneville may allow lamprey to be capable of free swimming. The bollard field at John Day was installed and designed to dissipate high velocity flows and to attract lamprey to a region of lower velocity. However, the bollard field creates high turbulence while dissipating velocity and this turbulence may generate upwelling and lateral forces that may stimulate lamprey to attach to the substrate to avoid being swept downstream. Questions regarding how lamprey alter their swimming and attachment behaviors under different hydraulic conditions (i.e. velocity and turbulence) will be explored further in a 2014 study in an experimental fishway at Bonneville Dam. Limited observations of attachments at Bonneville Dam may have been a function of limited DIDSON coverage of the fishway floor or other surfaces suitable for attachment in high velocity segments, particularly at NDE. It is likely that attachment events occurred but were not within the field of observation.

Vertical distributions

In past studies, lamprey are considered to be primarily a demersal species that orients to hard substrates and surfaces such as the fishway floors in high velocity areas (Moser et al. 2007; Keefer et al. 2011). In the Bonneville transition area, however, lamprey were observed more frequently in the upper sample volumes of the water column in the two deployments (JPU_LONG, JPU_SHORT) at the second weir. We think a likely explanation for this pattern is that water velocity was relatively low in the transition area, allowing free-swimming, as has been observed in locations such as count windows. Transition areas are known for variable flow conditions that are challenging for salmon passage (e.g., Naughton et al. 2007; Keefer et al. 2008), particularly at the location of the first weirs encountered by upstream migrating fish because these weirs are often fully submerged by elevated tailrace conditions, markedly reducing water velocities in an area with increased structural complexity created by the weirs. Our DIDSON-based water velocity estimates (0.24-0.43 m/s) from the Bonneville transition area suggest hydraulic cues may be inadequate for effective upstream guidance. Thus, understanding the distribution and behavior of lamprey as they first encounter and attempt to pass this segment was a high priority in 2013.

Our results suggest that many lamprey are in the lower water column as they approach the first submerged weir of the transition area (JPU_XSECT), where sturgeon densities are also higher. This observation contrasts with our observations from the junction pool in 2012 where lamprey densities were greater in upper sample volumes and sturgeon were lower in the water column (Johnson et al. 2013). The 2012 junction pool location was just downstream from the transition area surveyed in 2013 (Figure 28). In combination, these results suggest adult lamprey may alter their relative vertical distribution in the ~15m between the area sampled in the junction pool in 2012 and the first weir sampled in 2013. This behavior may be a response to subtle hydraulic cues as the channel narrows, or changes in the upwelling characteristics of flow fields since the entire fishway floor is composed of diffuser grating in this reach. Additionally, this observation may be an artifact of the upwardly sloping floor at these locations, which would cause lamprey travelling at constant depth to move closer to the floor (and sturgeon) as they moved upstream from the junction pool to the first weir (see Figure 28). Future analyses comparing absolute depth of lamprey could partially address these hypotheses.

Figure 28. Bonneville Dam junction pool and transition area looking upstream from the NDE collection channel toward Weir 8. The red and yellow lines represent the approximate locations of the I-beams that the DIDSON was deployed onto. DIDSON deployments in the junction pool from 2012 were made on the yellow line in the near-field with the sample volume capturing the area approximately above the square of diffuser grating in the lower left corner of the diffuser grating field. 2013 deployments in the transition area were made on the red line at the overflow weirs.

Since flow through the lower weir orifices when the weirs are inundated, lamprey likely move to the upper water column where hydraulic cues are stronger to guide them upstream over the second weir. This hypothesis is consistent with the observation of higher densities of lamprey in the upper sample volumes between the first and second weirs (JPU_SHORT and JPU_LONG) and it is also consistent with a predator avoidance mechanism at this location since sturgeon densities were higher in the lower sample volumes between the weirs. Hence, lamprey behavior at the overflow and orifice weir sections in the fish ladder may vary both temporally (i.e., as tailwater elevation changes) and spatially (i.e., with distance up the ladder). We also believe the vertical distribution of lamprey in the transition area is affected by additional structural (e.g. diffuser grating) and predator cues (e.g. sturgeon presence).

Lamprey were observed at higher rates in the sample volumes of the lower water column for all deployment locations at John Day, which is consistent with our original expectation that lamprey become increasing demersal as water velocity increases. Differential use of the water column between Bonneville and John Day was also observed in 2012. One potential hypothesis to explain this distribution is that lamprey preferentially select upstream routes with the lowest available velocities through a given cross section of fishway, as observed in an experimental flume (Keefer et al. 2011). Given the water velocity estimates from the DIDSON data at NDE (0.46-1.16 m/s), we hypothesize that the reduced nighttime velocities at Bonneville Dam may encourage lamprey to swim freely in the open water column rather than orient to the bottom. In contrast, velocity reductions in the north fish ladder at John Day are achieved through the bollard field, which dissipates the high velocity along the fishway floor near the entrance, but maintains relatively high velocities between the transition area and fishway entrance. Upstream of the bollard field, velocities are also expected to be lowest near the floor and fishway wall due to both edge effects and upwelling water through the fishway floor. Hence, lamprey may orient to those lower velocity fields along the bottom during upstream movements through the higher velocities inside the John Day North Fishway entrance.

Fish orientation and upstream-downstream movements

Our observations of fish depth and orientation provide qualitative insights regarding lamprey behavior, while directional movements provide a more quantitative measure regarding the rate of net upstream and downstream movements in the fishways. Most lamprey observations at Bonneville Dam were of fish orienting upstream. The NDE_LFS deployments had high proportions of both upstream orientations and upstream movements, which suggests that the environmental or hydraulic cues near the LFS entrance slot are sufficient for guiding fish to this area. At the NDE_UP deployment, however, a large proportion of fish that were initially observed oriented upstream had changed to a downstream orientation by the time of their last observation. A potential explanation for this pattern is that fish approached and failed to pass through the high velocities near the entrance. Fishway entrances and the high velocities at these locations have been implicated as a potential passage barrier for lamprey (Moser et al. 2002b; Johnson et al. 2012a). Swimming performance and water speed estimates also support this hypothesis. Higher water velocities were observed at NDE_UP (1.16 m/s during reduced night-time velocity) than at NDE_DOWN (0.76 m/s), suggesting that velocities increased closer to the entrance. The tail-beat frequency estimates for fish at NDE_UP (4.03 beats/s; Figure 18) were also higher than the estimates at NDE_LFS_UP (2.22 beats/s), which did not have an associated change in net upstream orientations (Figure 11).

Estimates of the proportion of upstream movements were lower in the transition area than at NDE. Given the high event rates for the transition area deployments, particularly in the upper water column, it is likely that some fish were observed multiple times swimming upstream and downstream past the DIDSON. These observations are concordant with radiotelemetry studies that showed the transition area was associated with high turn-around and multiple passage attempt rates by lamprey (Keefer et al. 2013c). In contrast, the orientation of fish in the lower water column was often in the lateral direction across the fishway channel and involved little overall net upstream or downstream movement. These “milling behaviors” may be in response to the predatory sturgeon that appeared to congregate near the first two weirs in the transition area and/or limited attraction flow in the lower water column, including through the submerged weirs.

At John Day, the majority of events at all deployment locations involved fish oriented upstream, but proportionately more movements were downstream than at Bonneville Dam. These observations suggest that although a large number of fish are orienting upstream, the overall progress of a significant number of those fish is in the downstream direction. One potential explanation for this observation is that lamprey struggle to move upstream against the high velocities within the north fishway collection channel, which results in an overall net downstream movement. Lamprey may also be actively initiating downstream movements due to some other behavioral decision as lamprey have been qualitatively observed to move quickly downstream, while orienting upstream.

In our 2012 and 2013 studies, we observed that downstream movements tended to be more frequent in the sample volumes of the upper water column than the lower water column at John Day Dam. Lamprey that are actively moving downstream may move upward in the water column to reduce the probably of collisions with structures and/or encounters with predators (especially sturgeon), as few rheotactic or olfactory cues would be available during downstream movements relative to upstream movements. Lamprey may also passively drift downstream in the plumes observed in the upper water column to minimize energy expenditure in their downstream movements. In contrast, proportionally more upstream movements were observed in the lower water column, which again, may reflect lower water velocities along the fishway floor or a greater availability of attachment surfaces for lamprey.

We observed some differences between years at John Day Dam which may have been related to interannual differences in operations there. In our 2012 study, no net upstream movement was observed in the upper or lower water column at JD3, while the net upstream movement at JD1 in 2012 was positive in the lower water column (~0.6) and negative in the upper water column (~ -0.6) (Johnson et al. 2013). In our 2013 study, similar patterns of upstream and downstream movements were observed at JD1, while the net upstream movement at JD3 was substantially higher. Additionally, the net upstream movement at JD5_XSECT in 2013 was much higher than any estimates in 2012. Modifications in the lower fishway channel at John Day that began in the spring of 2012 were not completed until the spring of 2013. As a result, higher flow volumes were maintained through the diffusers in the lower collection channel near JD1 and JD3 during the 2012 run season, since the modifications were not completed until 2013 (M. Zyndol, *personal communication*). If the reduced flows in the lower channel in 2013 created better conditions for lamprey passage, this may explain the higher event rates and higher proportions of upstream movements observed in the lower collection channel in our 2013 study.

Sturgeon distributions and associations with lamprey

Although lamprey and sturgeon were observed occupying the same part of the water column together, we never observed high lamprey event rates with high sturgeon event rates (with the exception of moderate rates of both at JPU_XSECT). This may indicate that lamprey were engaging in predator-avoidance behaviors. Anecdotally, we observed several lamprey at the JPU_LONG deployment in the transition area cease upstream movements and quickly move downstream or exit the frame of view in the presence of sturgeon. If this was, in fact, a predator-avoidance response, it is likely that chemoreception or vibrational cues detected by mechanoreceptors may be important for detecting sturgeon. Lamprey species have highly developed olfactory systems (Yun et al. 2011), and recent studies have shown aversion to odors associated with lamprey injury and mortality (e.g., Imre et al. 2010; Wagner et al. 2011). There has also been speculation that lamprey respond to potential chemical barriers associated with new passage structures, further suggesting lamprey may respond to olfactory cues within their environment (Jepson et al. 2011; Moser et al. 2011). If chemoreception of predator cues affects lamprey behavior, the olfactory environment in the transition area will be complex and impacted by the distribution of sturgeon, flow patterns, and attraction cues pumped through diffuser grating in the fishway floor.

At John Day dam, lamprey and sturgeon occupied the lower water column together in the lower fishway segments near the fishway entrance and very few lamprey were observed in the transition area where sturgeon activity was highest. Hence, white sturgeon may have varying effects on lamprey behavior depending on flow conditions. Y-maze experiments have been proposed to test the olfactory recognition of predators by lamprey (Moser et al. 2010). If lamprey are shown to respond to the chemical cues from sturgeon or dead or injured lamprey, then more controlled experiments would be needed to determine if specific lamprey passage behaviors inside fishways (i.e. failure, turn-around rate) may be invoked by sturgeon and under what conditions. Understanding whether the distribution of lamprey is associated with poor hydraulic cues or high sturgeon density is important to evaluating potential fishway modifications that focus on either reducing encounters with sturgeon or improving fishway hydraulics for lamprey.

Lateral distributions

The lateral distributions at the JPU_LONG deployment in the transition area suggested that lamprey were fairly evenly distributed across the lateral plane when swimming upstream at this site. Higher event rates were also observed at the two cross-sectional deployments in the transition area compared with the deployment facing upstream along the north wall (JPU_SHORT). One likely explanation is that the distribution of lamprey is more diffuse in the transition area because low velocities and a consistent lateral flow field do not provide strong orientation cues that aggregate lamprey. A second potential explanation is that lamprey distribution is affected by the rate of exit from the three collection channels entering the junction pool. For example, we observed in 2012 that lamprey were less frequently observed along the north wall near the south entrance collection channels compared with the south wall near the NDE collection channel, which could explain the lower event rates along the north wall at JPU_SHORT.

At John Day, lateral distribution patterns in the lower collection channel were markedly different from those in the Bonneville transition area. All events in the lower water column at the John Day LPS deployment occurred within 2 m of the LPS and north wall, tentatively suggesting a guidance effect of the angled bollard field or sufficient attraction cues emitted from the LPS. The highest proportion of upstream events in the upper water column at JD5_XSECT occurred closest to the north fishway wall. In contrast, the lower water column deployment suggested a relatively uniform distribution of fish exiting the bollard field across the lateral plane. It is important to note that the JD5_XSECT deployment did not capture the north fishway wall and probably underestimates the full extent of lamprey activity at this location. These patterns are consistent with previous observations of lamprey where they oriented primarily to the walls and floors in an experimental flume (Keefer et al. 2010, 2011), and are similar to the patterns we observed in the 2012 DIDSON study. Water velocity likely affects whether lamprey orient towards the fishway walls and floors, especially if lamprey employ their attachment behaviors specifically under high velocity conditions.

Late season deployments

The late season deployments at the Bonneville Dam transition area suggested that lamprey behavior was similar early and late in the run. The lower event rates at JPU_SHORT were likely a result of the declining abundance in the fish run. At JPU_XSECT_LATE, the slightly higher proportion of fish orienting upstream later in the run may be a result of the higher passage success of late season fish that may be associated with increased physiological performance or motivation (Keefer et al. 2009, 2013b). Changes in tailwater elevation may also affect movement or behavioral patterns in the transition area if orientation cues are stronger in guiding lamprey to the orifices. These temporal changes in behaviors would not be surprising given that temporally shifting bottlenecks have been observed at Bonneville Dam (Keefer et al. 2013c). The limited sample dates and inconsistency with previous deployments also limits the implications of these results.

Swim speed and tail-beat frequency estimates

A new component to the 2013 DIDSON study was to estimate water velocities, lamprey ground speeds, and tail beat frequencies from DIDSON imagery. These were relatively new approaches conducted primarily as an exercise to assess the applicability and validity of the methods. Several assumptions need to be addressed for these analyses. First, since the DIDSON integrates data from a three-dimensional volume into a two-dimensional image, it provides no information on the depth (z-axis) of fish or particles. Hence, we assumed that the depth distribution of particles and fish changed minimally and their path was coplanar to the image field. Second, we treated all particles as moving passively in the current regardless of type (i.e. entrained air bubbles, debris, sediment). Violation of either assumption would cause an underestimation of velocity.

Only one previous study has reported measuring water velocities using a DIDSON. Deng et al. (2009) conducted an experiment in a laboratory flume where the velocities of identifiable objects introduced into the flow fields were calculated. Their estimates were comparable to the measurements they made using laser doppler velocimetry (LDV). Our DIDSON-based estimates at the NDE_UP deployment (1.16 m/s) are similar to the target reduced nighttime velocities that are currently implemented at Bonneville for improving lamprey passage (mean target velocity at entrances = 1.20 m/s) (Johnson et al. 2012a; Moser et al. 2002b), which have been confirmed from hydraulic evaluations conducted at the NDE entrance and in the collection channel (Hydraulic evaluation, 2005; S. Schlenker, *personal communication).* The DIDSON estimates at NDE_DOWN (0.76 m/s) were slightly lower, which was likely a result of flow dissipating into the tailrace. The velocity estimates for NDE_LFS_UP (0.46 m/s) in the lower water column below the fishway entrance plume were much lower than the other two NDE deployments. Velocity estimates in the transition area were low, which was likely a result of the large cross-sectional area of water above the submerged weirs in the lower transition area. Simulated models of velocity at the Washington-shore junction pool suggest that our velocity estimates at JPU_LONG (0.32 m/s) and JPU_XSECT (0.43 m/s) were reasonably similar to observed velocities at this site (0.46-1.00 m/s; dependent upon tailwater elevation) (Hydraulic Evaluation, 2005).

Swim speed estimates and tail-beat frequencies offer potential methods for making inferences about the energy expenditure of fish (Hinch and Rand 2000; Mueller et al. 2010). A previous study concluded that fish ground speeds could be accurately calculated from DIDSON imagery, but was dependent upon the orientation of the DIDSON and swim path of the fish (Mueller et al. 2008). This is why we selected fish with only a relatively linear trajectory in the horizontal direction and camera deployments where movement appeared coplanar. Importantly, tail beat frequencies do not have to make assumptions regarding movement in the z-direction (depth) and are more directly linked to physiology than swim speed (Mueller et al. 2010). The unexplained variation observed in the relationship between TBF and swim speed through the water (Figure 19) was probably related to two factors. The first is measurement error related to non-coplanar movement of lamprey or particles, or non-passive movement of particles. The second substantial source of variation may have been related to lamprey size because swim speed increases in large fish for a given TBF. Future analyses could correct for the latter source to some degree by estimating size of lamprey from DIDSON imagery.

Our swim speed data suggest lamprey may be swimming at or above their critical swim speed because the swim speeds through water observed across all deployment locations (Figure 17c) were near or above the critical swim values observed by Mesa et al. (2003) in a swim tunnel (range: 0.81-0.86 m/s). Critical swim speed is defined as the maximum sustainable swim speed that fish can maintain for a prolonged period of time and is considered a robust measure of both swimming endurance and aerobic capacity (Mesa et al. 2003; Katopodis and Gervais 2012). Interestingly, the ground speed estimates for lamprey differed minimally between NDE and transition area deployments despite difference in estimated water velocities. Although ground speeds did not differ between locations, the higher swim speeds through water at NDE suggest that lamprey likely work harder to maintain those ground speeds near the fishway entrance.

The positive correlation between tail beat frequency and lamprey swim speeds through water (Figure 19) suggests that TBF can be estimated from swim speeds, and vice versa. Our TBF calculations fell within the observed range of estimates for other fish species (Steinhausen et al. 2005; Mueller et al. 2010), suggesting our estimates were reasonable. The poor passage of lamprey versus Pacific salmon and steelhead is hypothesized to result from swimming differences between the species, since salmonids have higher burst speeds and higher endurance compared to lamprey and other anguilliform swimmers (Katopodis and Gervais, 2012). The potential for quantifying TBF for lamprey within fishway environments has important potential future applications implications. For example, using DIDSON to estimate TBFs for lamprey at specific locations within the fishways can identify whether problem passage areas are associated with constraints related to endurance barriers (i.e., long segments requiring swimming just above the critical swim speed) or burst swimming barriers (i.e., segments with water velocity exceeding the swimming capacity of lampreys). This approach provides an additional tool for developing insights regarding the relationship between the swim speed and energetic expenditure of fish within fishway environments using direct in situ observations.

In our opinion, TBF estimates were likely the more accurate and applicable stand-alone metric in comparison to the estimates of water velocity and swim speed. Considering the differences we observed between NDE and the transition area, tail-beat frequencies may be more useful for detecting differences in the swimming performance of lamprey than ground speeds. The methods for calculating TBF's from DIDSON imagery also has been addressed more thoroughly in the scientific literature, thereby strengthening its applicability (Mueller et al. 2010). In contrast, the ground speed and water velocity estimates require several assumptions that potentially limit confidence in these results. These methods should be corroborated using laboratory and field studies that measure water velocities and lamprey swim speeds. Future measurements of TBF under controlled conditions, including the TBF associated with critical and maximum swim speeds could be used in conjunction with *in situ* DIDSON observations to directly estimate the energetic costs of passage in various fishway locations.

Conclusion

The DIDSON has provided an effective, non-invasive tool for monitoring some aspects of Pacific lamprey passage inside fishways. The 2013 results have shown that Pacific lamprey distribution and movements may be more complex than previously thought. Lamprey appear to exhibit a variety of behaviors depending upon the biological (i.e. sturgeon presence), hydraulic (i.e. velocity and turbulence), and structural (i.e. bollard fields) conditions encountered within the fishways. We have also tested several novel methods for estimating lamprey swimming performance that could provide additional information on the fishway passage behaviors of this species. Overall, the future application of the DIDSON will be most successful for making behavioral observations of species that should be handled minimally (i.e. endangered species) under conditions where traditional, optical video is limited or active telemetry studies are not feasible.

References

Belcher, E. O., H. Q. Dinh, D. C. Lynn and T. J. Laughlin. 1999. Beam forming and imaging with acoustic lenses in small, high-frequency sonars. OCEANS, 1999. MTS/IEEE Conference and Exhibition.

Belcher, E. O., B. Matsuyama and G. Trimble. 2001. Object identification with acoustic lenses. OCEANS, 2001. MTS/IEEE Conference and Exhibition.

Boswell, K. M., M. P. Wilson, J. H. Cowan, Jr. 2008. A semi automated approach to estimating fish size, abundance, and behavior from dual-frequency identifications sonar (DIDSON) data. North American Journal of Fisheries Management 28:799-807.

Breder, C. M. 1926. The locomotion of fishes. Zoologica 4:159-256.

Caudill, C. C., W. R. Daigle, M. L. Keefer, C. T. Boggs, M. A. Jepson, B. J. Burke, R. W. Zabel, T. C. Bjornn, and C. A. Peery. 2007. Slow dam passage in Columbia River salmonids associated with unsuccessful migration: delayed negative effects of passage obstacles or condition–dependent mortality? Canadian Journal of Fisheries and Aquatic Sciences 64:979–995.

Clabough, T. S., M. L. Keefer, C. C. Caudill, E. L. Johnson, and C. A. Peery. 2012. Use of night video to enumerate adult Pacific lamprey passage at hydroelectric dams: challenges and opportunities for improved escapement estimation. North American Journal of Fisheries Management 32:687-695.

Columbia Basin Research, School of Aquatic & Fishery Sciences, University of Washington. 2013. Columbia River DART (Data Access in Real Time). Retrieved March 9, 2014, from http://www.cbr.washington.edu/dart.

Deng, Z. R., P. Mueller, and M. C. Richmond. 2009. Measuring water velocity using DIDSON and image cross-correlation techniques. In *Waterpower XVI: New Roles for Hydro in a Changing World, July 27-30, 2009, Spokane, Washington*, p. Paper No. 130. US Army Corps of Engineers, Washington DC.

Fay, R. R., and A. M. Simmonds. 1999. The sense of hearing in fishes and amphibians. In: Comparative hearing: fishes and amphibians. Pp. 269-318. In: Fay, R. R. and A. N. Popper (eds). Springer-Verlag, New York.

Hinch, S. G., and P. S. Rand. 1998. Swim speeds and energy use of upriver-migrating sockeye salmon (*Oncorhynchus nerka*): role of local environment and fish characteristics. Canadian Journal of Fisheries and Aquatic Sciences **55**: 1821–1831.

Holmes, J. A., G. M. W. Cronkite, H. J. Enzenhofer, and T. J. Mulligan. 2006. Accuracy and precision of fish-count data from a “dual-frequency identification sonar” (DIDSON) imaging system. ICES Journal of Marine Science 63:543-555.

Imre, I., G. E. Brown, R. A. Bergstedt, and R. McDonald. 2010. Use of chemosensory cues as repellents for sea lamprey: potential directions for population management. Journal of Great Lakes Research 36:790-793.

Jepson M. A., M. L. Keefer, C. C. Caudill, and B. J. Burke. 2011. Passage behavior of adult Spring Chinook salmon at Bonneville Dam including evaluations of passage at the modified Cascade Islands fishway, 2010. UI FERL report 2011-1-Technical Report for the US Army Corps of Engineers, Portland District.

Johnson, E. L., C. C. Caudill, T. S. Clabough, M. L. Keefer, M.A. Jepson, and M. L. Moser. 2010. Effects of lowered fishway water velocity on fishway entrance success by adult Pacific lamprey at Bonneville Dam, 2007-2009. Technical report 2010-4 of Idaho Cooperative Fish and Wildlife Research Unit to U.S. Army Corps of Engineers, Portland District.

Johnson, P. N. and B. Le. 2011. Assessment of adult Pacific Lamprey response to velocity reductions at Wells Dam fishway entrances (DIDSON Study Report). Wells Hydroelectric Project, FERC NO. 2149. Final technical report submitted to Douglas County Public Utility District No. 1, East Wenatchee, Wash.

Johnson, E. L., C. C. Caudill, M. L. Keefer, T. S. Clabough, M. A. Jepson, and M. L. Moser. 2012a. Movement of radio-tagged adult Pacific lamprey during a large-scale fishway velocity experiment. Transactions of the American Fisheries Society 141:571-579.

Johnson, E. L, T. S. Clabough, M. L. Keefer, C. C. Caudill, P. N. Johnson, W. T. Nagy, and M. A. Jepson. 2012b. Evaluation of Dual-Frequency Identification Sonar (DIDSON) for Monitoring Pacific Lamprey Passage Behavior at Fishways of Bonneville Dam, 2011. Technical Report 2012-5 of Idaho Cooperative Fish and Wildlife Research Unit to U.S. Army Corps of Engineers, Portland District.

Johnson, E. L., T. S. Clabough, M. L. Keefer, C. C. Caudill, P. N. Johnson, M. A. Kirk, and M. A. Jepson. 2013. Evaluation of dual-frequency identification sonar (DIDSON) for monitoring Pacific lamprey passage behavior at fishways of Bonneville and John Day dams, 2012. UI FERL report 2013-5-DRAFT for the US Army Corps of Engineers, Portland District.

Johnson, P .N., C. C. Caudill, E. L. Johnson, T. S. Clabough, C. T. Boggs, W. T. Nagy, and M. L. Keefer. *In review*. Use of Dual-Frequency Identification Sonar (DIDSON) to monitor adult Pacific lamprey at dam fishways: Deployments, data interpretation, and inter-observer effects.

Katopodis, C. and R. Gervais. 2012. Ecohydraulic analysis of fish fatigue data. River Research and Applications 28: 444-456.

Keefer, M. L., D. C. Joosten, C. L. Williams, C. M. Nauman, M. A. Jepson, C. A. Peery, T. C. Bjornn, R. R. Ringe, K. R. Tolotti, S. R. Lee, L. C. Stuehrenberg, M.L. Moser, and B. J. Burke. 2008. Adult salmon and steelhead passage through fishways and transition pools at Bonneville Dam, 1997-2002. Technical Report 2008-5 of Idaho Cooperative Fish and Wildlife Research Unit to U.S. Army Corps of Engineers, Portland District.

Keefer, M. L., M. L. Moser, C. T. Boggs, W. R. Daigle, and C. A. Peery. 2009. Variability in migration timing of adult Pacific lamprey (*Lampetra tridentata*) in the Columbia River, U.S.A. Environmental Biology of Fish 82: 253-264.

Keefer, M. L., W. R. Daigle, C. A. Peery, H. T. Pennington, S. R. Lee, and M. L. Moser. 2010. Testing adult Pacific lamprey performance at structural challenges in fishways. North American Journal of Fisheries Management 30:376-385.

Keefer, M. L., C. A. Peery, S. R. Lee, W. R. Daigle, E. L. Johnson, and M. L. Moser. 2011. Behavior of adult Pacific lampreys in near–field flow and fishway design experiments. Fisheries Management and Ecology 18:177–189.

Keefer, M. L., C. C. Caudill, C. A. Peery, and M. L. Moser. 2013a. Context-dependent diel behavior of upstream-migrating anadromous fishes. Environmental Biology of Fishes 96: 691-700.

Keefer, M. L., C. T. Boggs, C. A. Peery, and C. C. Caudill. 2013b. Factors affecting dam passage and upstream distribution of adult Pacific lamprey in the interior Columbia River basin. Ecology of Freshwater Fish 22:1-10.

Keefer, M. L., C. C. Caudill, T. S. Clabough, M. A. Jepson, E. L. Johnson, C. A. Perry, M. D. Higgs, and M. L Moser. 2013c. Fishway passage bottleneck identification and prioritization: a case study of Pacific lamprey at Bonneville Dam. Canadian Journal of Fisheries and Aquatic Sciences 70: 1551-1565.

Kemp, P. S., T. Tsuzaki, and M. L. Moser. 2009. Linking behavior and performance: intermittent locomotion in a climbing fish. Journal of Zoology 277:171-178.

Mesa, M. G., J. M. Bayer, and J. G. Seelye. 2003. Swimming performance and physiological response to exhaustive exercise in radio-tagged and untagged Pacific lamprey. Transactions of the American Fisheries Society 132:483-492.

Moser, M. L., P. A. Ocker, L. C. Stuehrenberg, and T. C. Bjornn. 2002a. Passage efficiency of adult Pacific lamprey at hydropower dams on the lower Columbia River, USA. Transactions of the American Fisheries Society 131:956–965.

Moser, M. L., A. L. Matter, L. C. Stuehrenberg, and T. C. Bjornn. 2002b. Use of an extensive radio receiver network to document Pacific lamprey (*Lampetra tridentata*) entrance efficiency at fishways in the Lower Columbia River, USA. Hydrobiologia 483: 45-53.

Moser, M. L., J. M. Butzerin, and D. B. Dey. 2007. Capture and collection of lampreys: the state of the science. Reviews in Fish Biology and Fisheries 17:45-56.

Moser, M. L., A. Jackson, and C. Caudill. 2010. Olfactory signaling in adult Pacific lamprey: potential chemical obstacles to upstream movement at Columbia Basin fishways. Research Proposal LMP-P-10 to U.S. Army Corps of Engineers, Portland District.

Moser, M. L, M. L. Keefer, H. T. Pennington, D. A. Ogden, and JE Simonson. 2011. Development of Pacific lamprey fishways at a hydropower dam. Fisheries Management and Ecology 18: 190-200.

Moursund, R. A., T. J. Carlson, and R. D. Peters. 2003. A fisheries application of a dual-frequency identification sonar acoustic camera. ICES Journal of Marine Science 60:678-683.

Mueller, A-M, T. Mulligan, and P.K. Withler. 2008. Classifying sonar images: can a computer-driven process identify eels? North American Journal of Fisheries Management 28: 1876-1886.

Mueller, A., D. L. Burwen, K. M. Boswell, and T. Mulligan. 2010. Tail-beat patterns in dual-frequency identification sonar echograms and their potential use for species specific identification and bioenergetics studies. Transactions of the American Fisheries Society 139:900-910.

Naughton, G. P., C. C. Caudill, C. A. Peery, T. S. Clabough, M. A. Jepson, T. C. Bjornn, and L. C. Stuehrenberg. 2007. Experimental evaluation of fishway modifications on the passage behavior of adult Chinook salmon and steelhead at Lower Granite Dam, Snake River, USA. River Research and Applications 23: 99-111.

Pipal, K. A., J. J. Notch, S. A. Hayes, and P. B. Adams. 2012. Estimating Escapement for a Low-Abundance Steelhead Population Using Dual-Frequency Identification Sonar (DIDSON). North American Journal of Fisheries Management 32: 880-893.

Ransom, B. H., T. W. Steig, and P. A. Nealson. 1996. Comparison of hydroacoustic and net catch estimates of Pacific salmon smolt (*Oncorhynchus spp.*) passage at hydropower dams in the Columbia River Basin. ICES Journal of Marine Science 53:477-481.

Smith, D.L., J. M. Nestler, G. E. Johnson, and R. A. Goodwin. 2010. Species-specific spatial and temporal distribution patterns of emigrating juvenile salmonids in the Pacific Northwest. Reviews in Fisheries Science 18: 40-64.

Sound Metrics Corp. DIDSON Sonar 101: Getting good images with DIDSON. Available: http://www.didson.com/SONAR101/sn_sonar101.html. (2012).

Standen, E. M., S. G. Hinch, M. C. Healy, and A. P. Farrell. 2002. Energetic costs of migration through the Fraser River Canyon, British Columbia, in adult pink (*Oncorhynchus gorbuscha*) and sockeye (*Oncorhynchus nerka*) salmon as assessed by EMG telemetry. Canadian Journal of Fisheries and Aquatic Sciences 59:1809–1818.

Steig, T. W., and T. K. Iverson. 1998. Acoustic monitoring of salmonid density, target strength, and trajectories at two dams on the Columbia River, using a split-beam scanning system. River Research 35:43-53.

Steinhausen, M. F., J. F. Steffensen, and N. G. Andersen. 2005. Tail beat frequency as a predictor of swimming speed and oxygen consumption of saithe (*Pollachius virens*) and whiting (*Merlangius merlangus*) during forced swimming. Marine Biology148: 197-204.

Tiffan, K. F., D. W. Rondorf, and J. J. Skalicky. 2004. Imaging fall Chinook salmon redds in the Columbia River with a dual-frequency identification sonar. North American Journal of Fisheries Management 24:1421-1426.

United States Army Corps of Engineers. 2005. Hydraulic Evaluation of Lower Columbia River Adult Bypass Systems: (HELCRABS), Bonneville Second Powerhouse Fish Evaluation Report. Portland District.

Wagner, C. M., E. M. Stroud, and T. D. Meckley. 2011. A deathly odor suggests a new sustainable tool for controlling a costly invasive species. Canadian Journal of Fisheries and Aquatic Sciences 68:1157-1160.

Yun S. S., A. J. Wildbill, M. J. Siefkes, M. L. Moser, A. H. Dittman, S. C. Corbett, W. Li, and D. A. Close. 2011. Identification of putative migratory pheromones from Pacific lamprey (*Lampetra tridentata).* Canadian Journal of Fisheries and Aquatic Science 68: 2194-2203.

Appendix A

Table A1. DIDSON camera parameters at the north downstream entrance (NDE) deployments at Bonneville in 2013. Orientation: FIXED = capturing one depth stratum.

Deployment location	*Date*	*Orientation*	*Tilt*	*Compass (degrees)*	*Aux. lens*	*Camera depth (m)*	*Tailrace elevation (m)*	*Camera start (m)*	*Camera range (m)*
NDE _LFS_UP									
	20-21 Jun	FIXED	-17	206	No	2.7	5.5	2.08	10
NDE _LFS_LOW									
	16-17 Jul	FIXED	-44	208	No	7.6	5.0	2.08	7.08
	17-18 Jul	FIXED	-44	206	No	7.6	4.9	2.08	7.08
NDE_UP									
	30-31 Jul	FIXED	0	256	No	3.0	4.4	2.08	7.08
NDE_DOWN									
	31-1 Aug	FIXED	0	55	No	3.0	4.5	2.08	7.08

Table A2. DIDSON camera parameters at the transition area (JPU_LONG) deployments at Bonneville in 2013. Orientation: TILT = tilting feature to capture more than one depth strata, FIXED = capturing one depth stratum.

Deployment location	*Date*	*Orientation*	*Tilt*	*Compass (degrees)*	*Aux. lens*	*Camera depth (m)*	*Tailrace elevation (m)*	*Camera start (m)*	*Camera range (m)*
JPU_LONG									
	30-1 Jul	TILT	10/-14	248	No	4.0	6.6	2.08	7.08
	2-3 Jul	TILT	10/-14	246	No	4.0	6.6	2.08	7.08
	21-22 Jul	TILT	10/-14	258	No	-	4.9	2.92	7.92
JPU_LONG									
	27-28 Jun	FIXED	-14	246	No	4.0	6.6	2.08	7.08
	18-19 Jul	FIXED	-14	246	No	-	4.9	2.08	7.08

Table A3. DIDSON camera parameters at the transition area (JPU_SHORT) deployments at Bonneville in 2013. Orientation: TILT = tilting feature to capture more than one depth strata, FIXED = capturing one depth stratum.

Deployment location	*Date*	*Orientation*	*Tilt*	*Compass (degrees)*	*Aux. lens*	*Camera depth (m)*	*Tailrace elevation (m)*	*Camera start (m)*	*Camera range (m)*
JPU_SHORT									
	29-30 Jun	TILT	0/-40	316	No	4.0	6.6	2.08	7.08
	3-4 Jul	TILT	0/-40	318	No	4.0	6.5	2.08	7.08
	20-21 Jul	TILT	0/-40	315	No	-	5.0	2.08	7.08
JPU_SHORT									
	28-29 Jun	FIXED	-40	289	No	4.0	6.5	2.08	7.08
	19-20 Jul	FIXED	-40	286	No	-	4.7	1.25	6.25
	30-31 Aug	FIXED	3 to 7	327	No	0.8	3.7	2.08	7.08
	31-1 Sep	FIXED	-21 to -29	296	No	0.8	3.7	2.08	7.08

Table A4. DIDSON camera parameters at the transition area (JPU_XSECT) deployments at Bonneville in 2013. Orientation: TILT = tilting feature to capture more than one depth strata, FIXED = capturing one depth stratum.

Deployment location	*Date*	*Orientation*	*Tilt*	*Compass(degrees)*	*Aux. lens*	*Camera depth (m)*	*Tailrace elevation (m)*	*Camera start (m)*	*Camera range (m)*
JPU_XSECT									
	4-5 Jul	TILT	0/-40	175	No	2.1	6.4	2.08	7.08
	5 Jul	TILT	0/-40	175	No	2.1	6.4	2.08	7.08
	7-8 Jul	TILT	0/-40	175	No	2.1	6.2	2.08	7.08
JPU_XSECT_LATE*									
	27-28 Aug	FIXED	-30	228	No	0.8	3.5	2.08	7.08
	28-29 Aug	FIXED	-7	243	No	0.8	3.6	2.08	7.08

*This was a late season deployment that was included only for late season comparisons. See results for more on this deployment.

Table A5. DIDSON camera parameters for all deployments at John Day (JD1, JD2, JD3, JD5, and JD6) in 2013. Orientation: TILT = tilting feature to capture more than one depth strata, FIXED = capturing one depth stratum.

Deployment location	*Date*	*Orientation*	*Tilt*	*Compass(degrees)*	*Aux. lens*	*Camera depth (m)*	*Tailrace elevation (m)*	*Camera start (m)*	*Camera range (m)*
JD1									
	24-25 Jul	TILT	+/-7	90	No	0.8	49.1	2.08	7.08
JD3									
	27-28 Jul	TILT	+/-14	31	No	2.1	49.2	2.08	7.08
JD4									
	13-14 Jul	TILT	+/-14	310	No	2.6	49.3	2.08	7.08
	14-15 Jul	TILT	+/-14	310	No	2.6	49.4	2.08	7.08
	23-24 Jul	TILT	+/-7	309	No	-	49.2	2.08	7.08
JD5_XSECT									
	11-12 Jul	TILT	7/-15	315	No	2.1	49.4	2.08	7.08
	12-13 Jul	TILT	7/-15	315	No	2.1	49.4	2.08	7.08
JD5_LPS									
	22-23 Jul	TILT	+/-7	324	No	1.2	49.4	4.17	9.17
JD5_FIXED									
	9-10 Jul	FIXED	-9	268	No	1.2	49.4	4.17	9.17
	10-11 Jul	FIXED	-12	268	No	2.1	49.4	2.5	7.5
JD6									
	25-26 Jul	TILT	+/-7	262	No	2.3	49.3	2.08	7.08
JD6									
	28-29 Jul	FIXED	-11	238	No	2.1	49.1	2.08	7.08

Appendix B

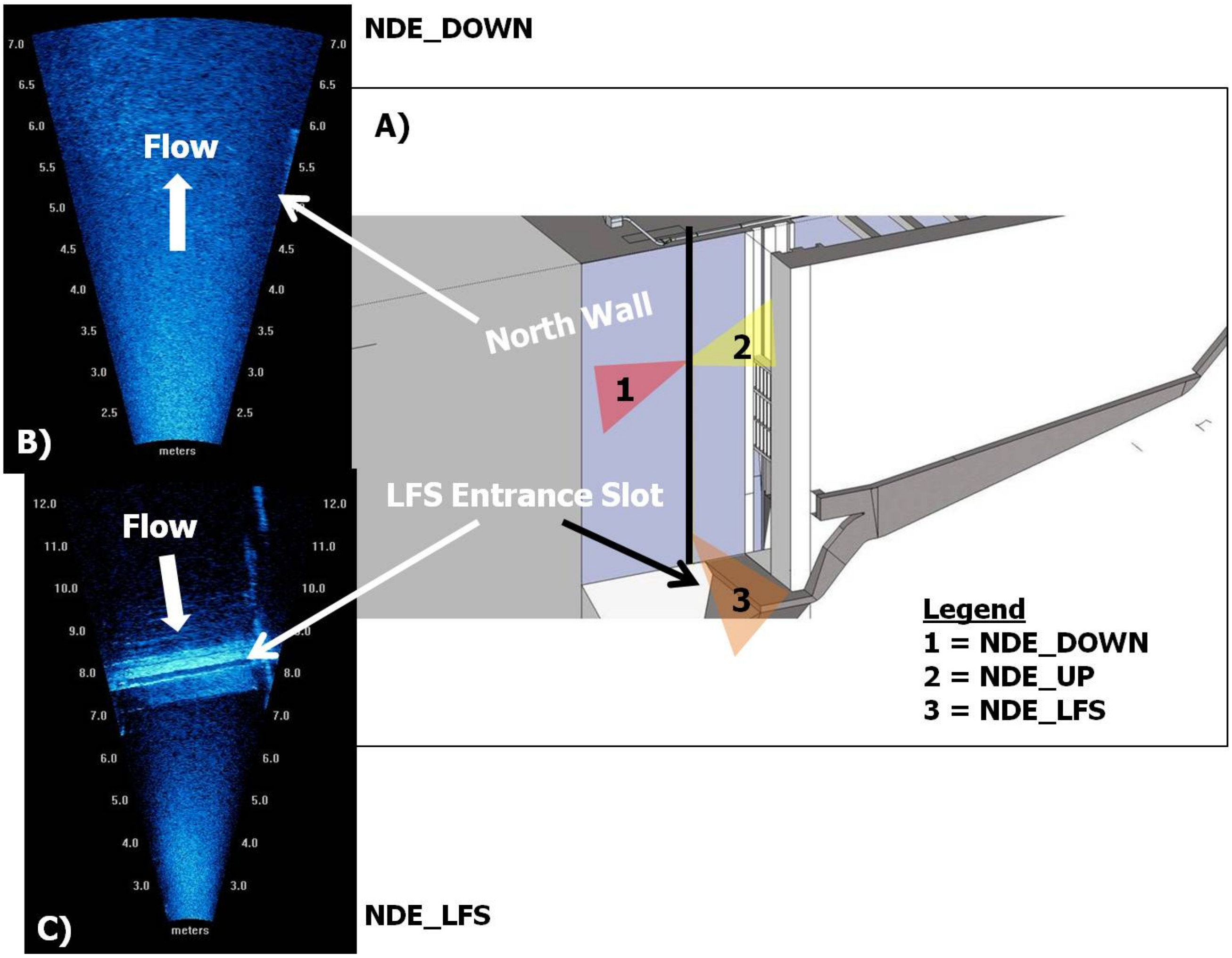

Figure 1. Deployments made at the north downstream entrance (NDE) location in 2013 at Bonneville Dam. (A) shows the location of the lamprey flume system (LFS) at the base of the fishway entrance and the entrance slot can be observed in the DIDSON footage (C).

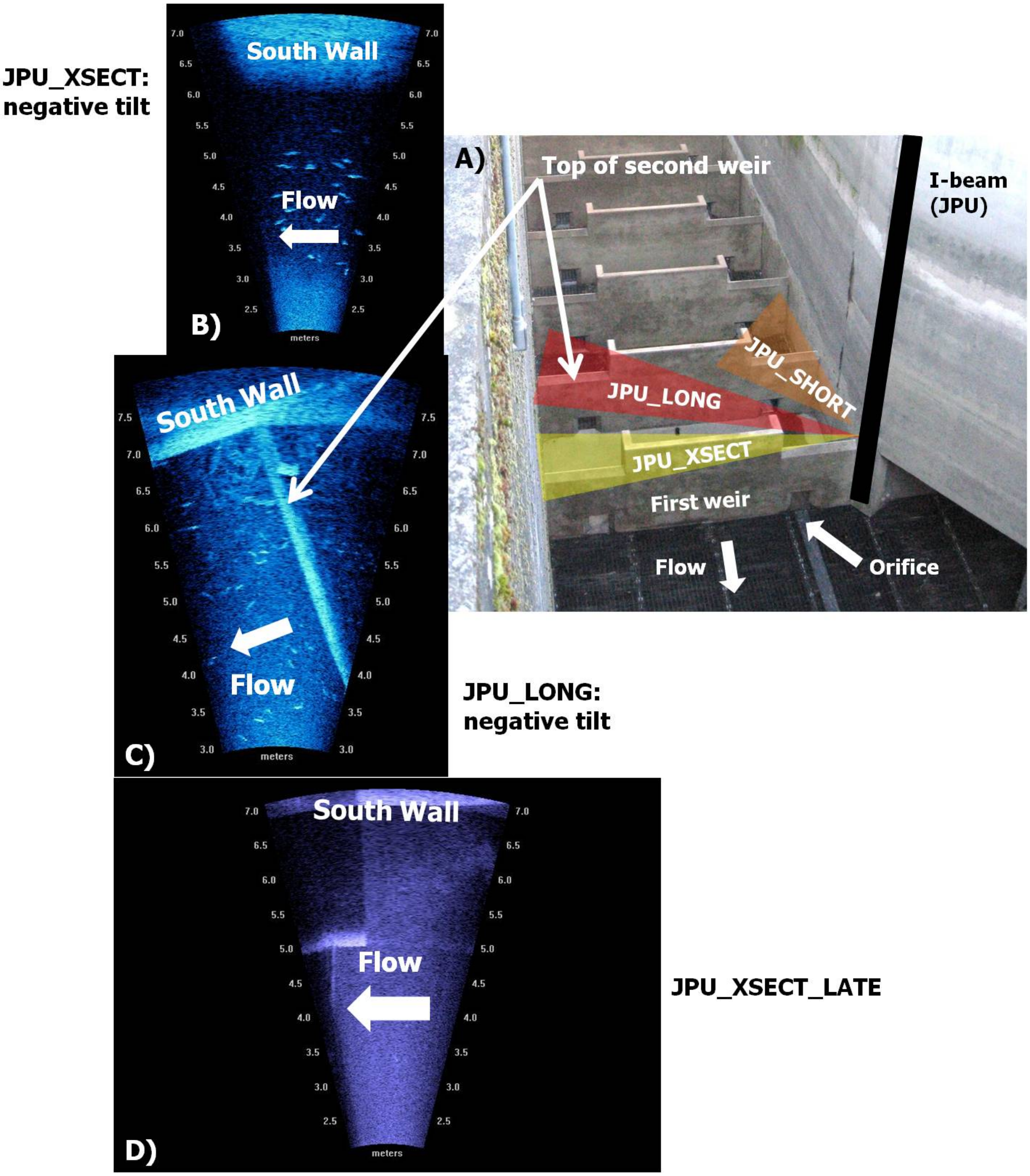

Figure 2. Deployments made at the transition area (JPU) in 2013 at Bonneville Dam and the DIDSON imagery captured for (B) JPU_XSECT, (C) JPU_LONG, and (D) JPU_XSECT_LATE. Figure 1 in the report provides an example of the images captured from the JPU_SHORT deployment.

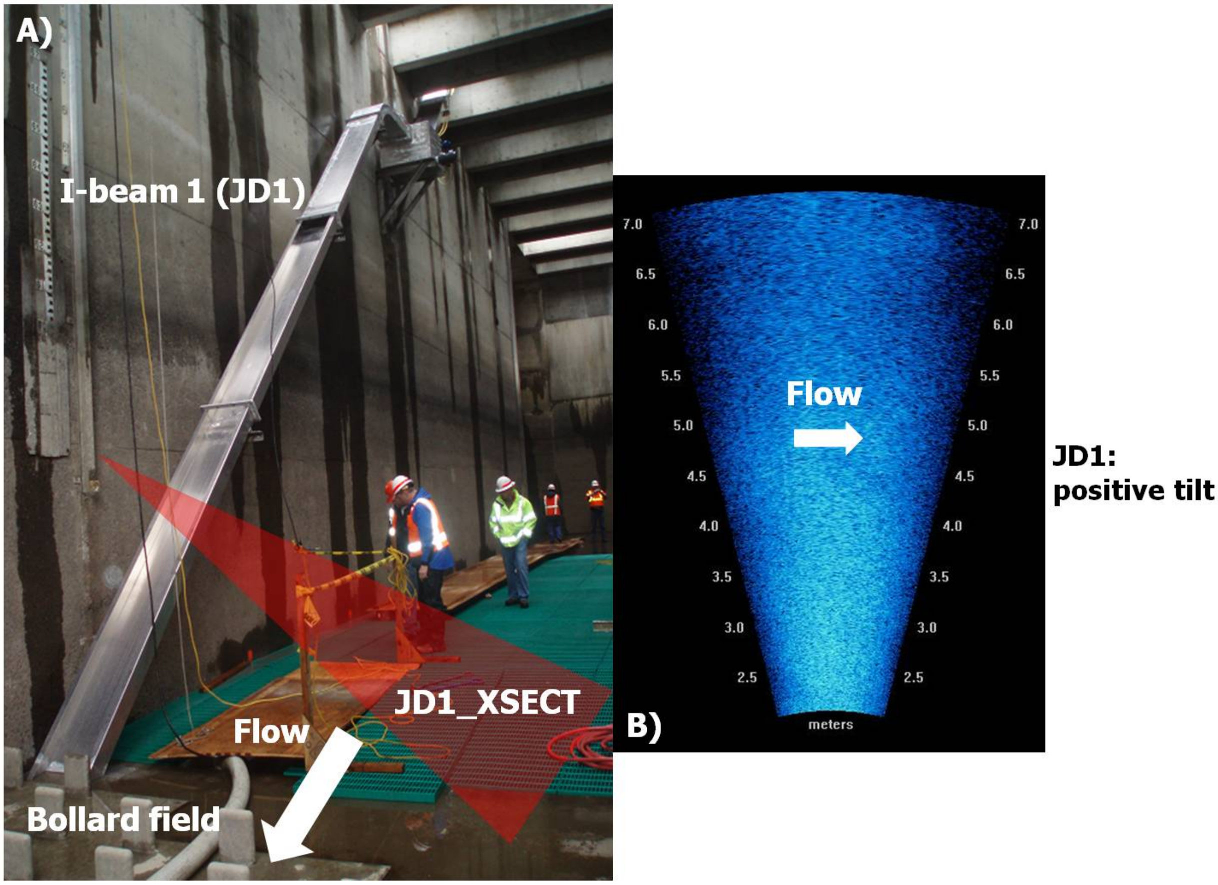

Figure 3. Deployment made at I-beam 1 (JD1) in 2013 at John Day Dam with (B) DIDSON imagery of the cross-sectional deployment at JD1.

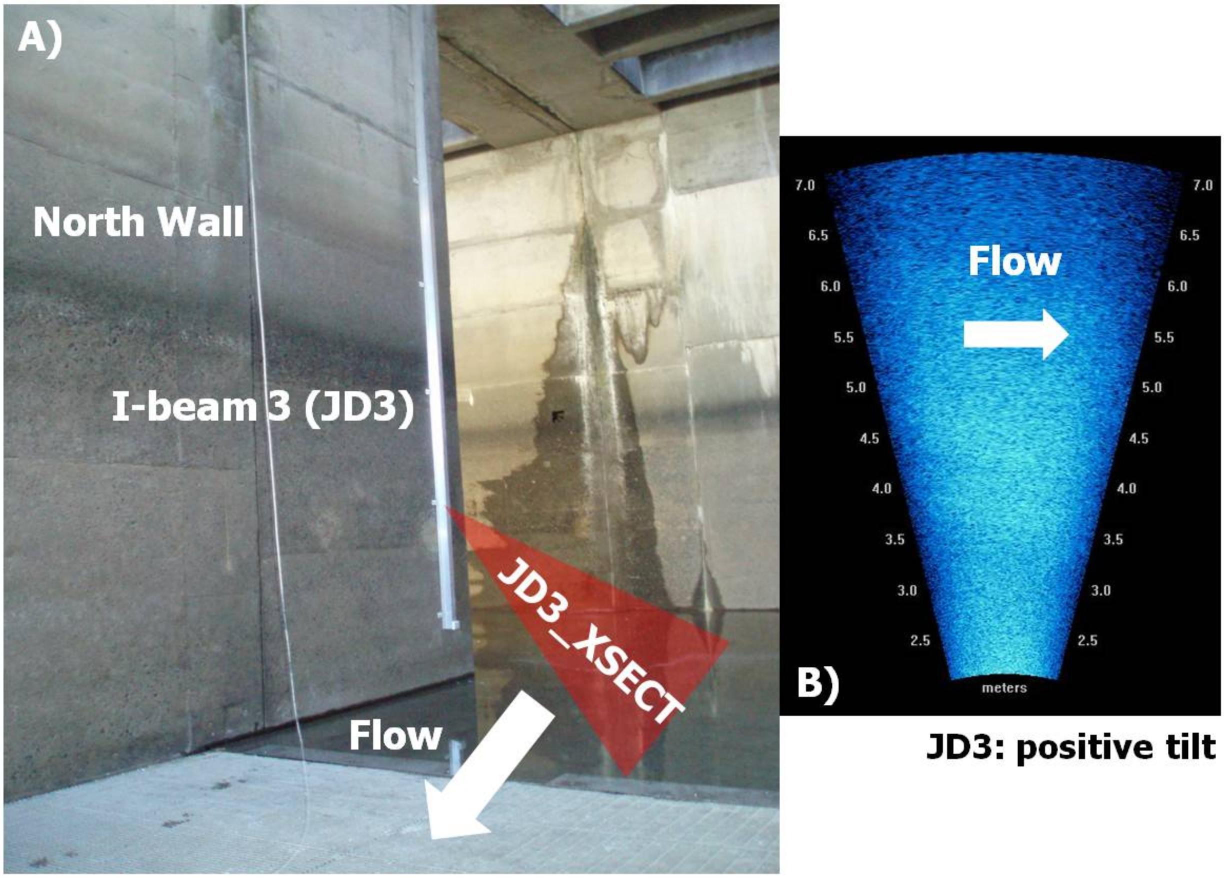

Figure 4. Deployment made at I-beam 3 (JD3) in 2013 near the turn pool at John Day Dam with (B) DIDSON imagery of the cross-sectional deployment at JD3.

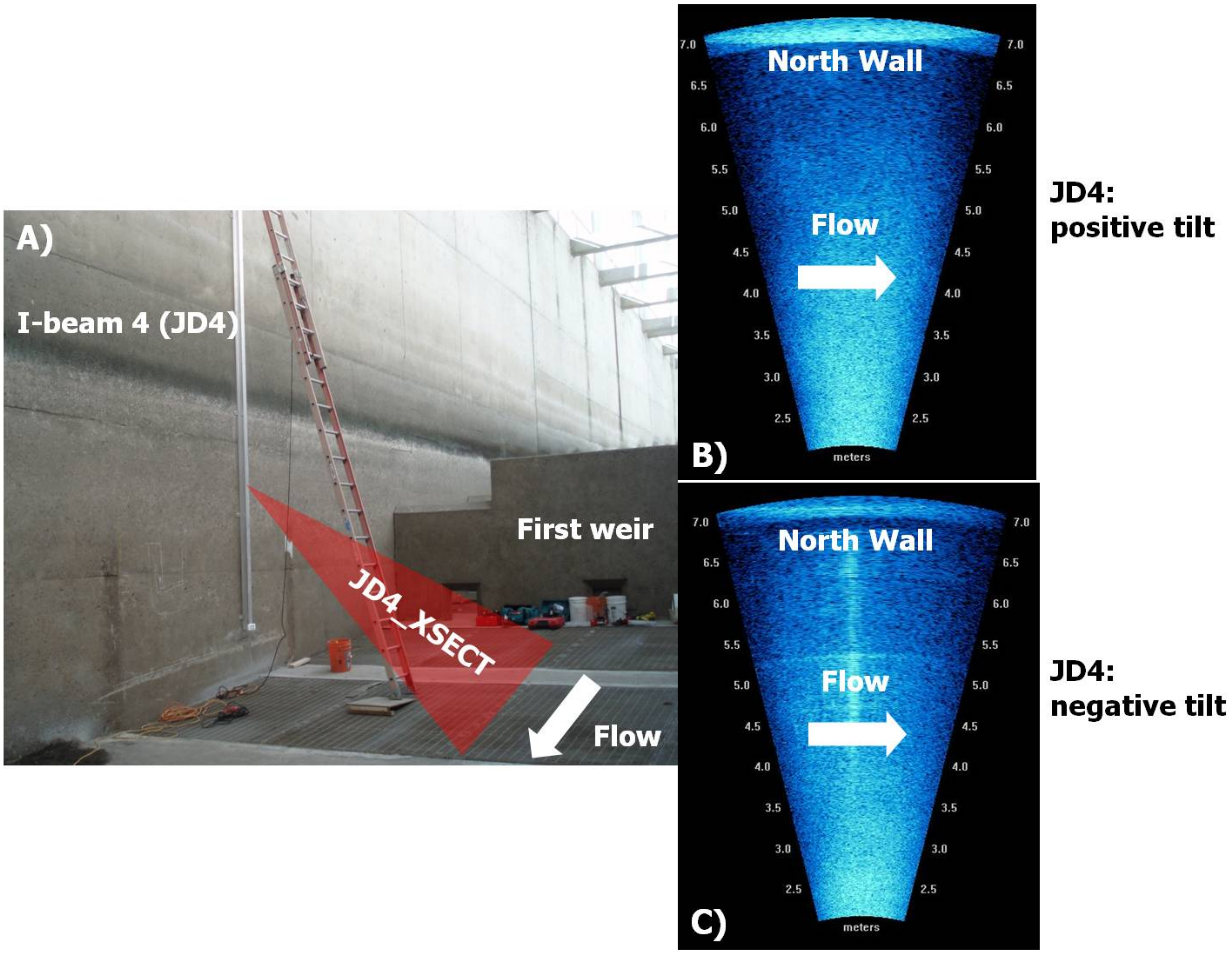

Figure 5. Deployment made at I-beam 4 (JD4) in 2013 at John Day Dam with (B) DIDSON imagery in the positive and (C) negative tilt of the cross-sectional deployment at JD4.

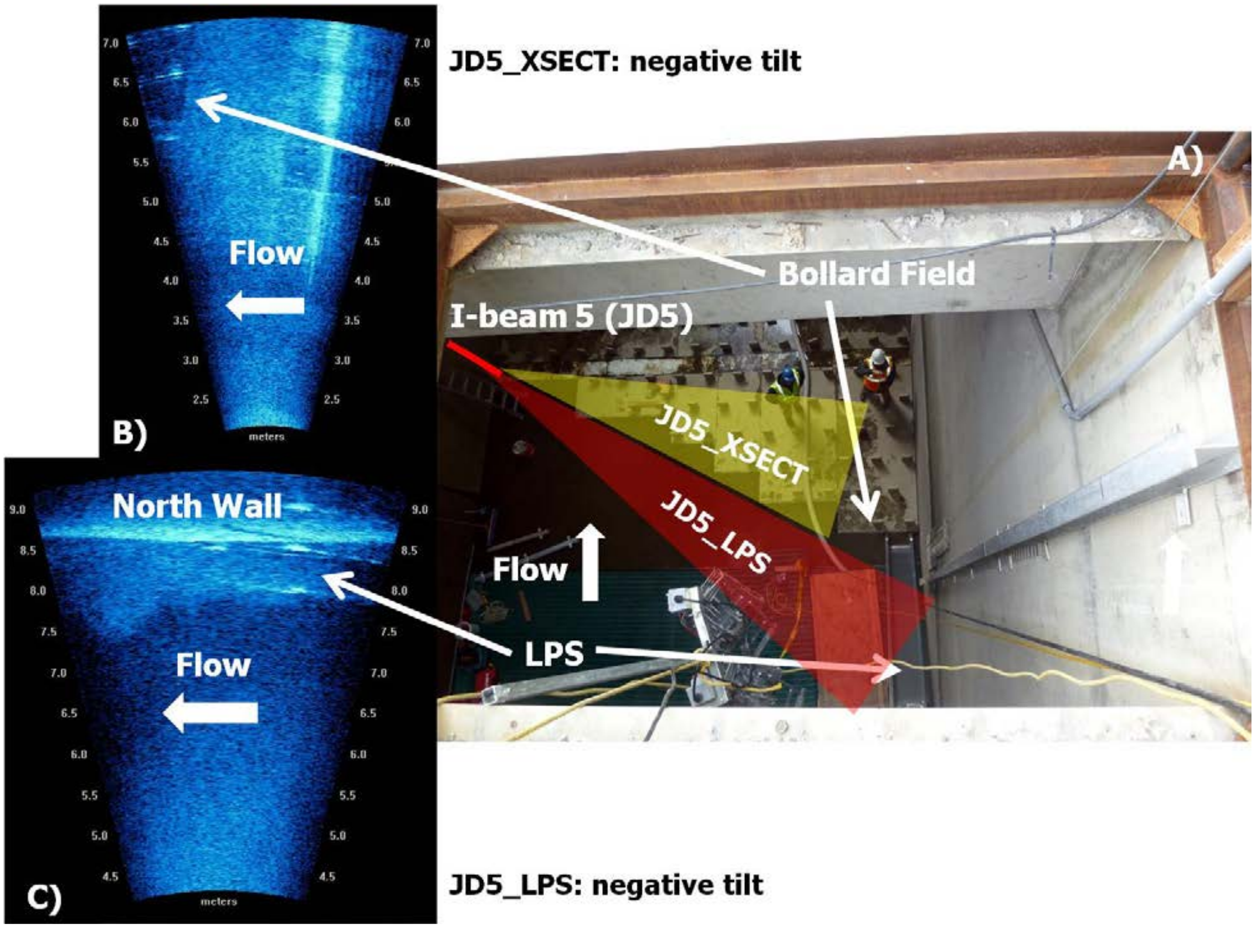

Figure 6. Deployment made at I-beam 5 (JD5) in 2013 at John Day Dam with (B) DIDSON imagery capturing the end of the bollard field and (C) imagery capturing the LPS.

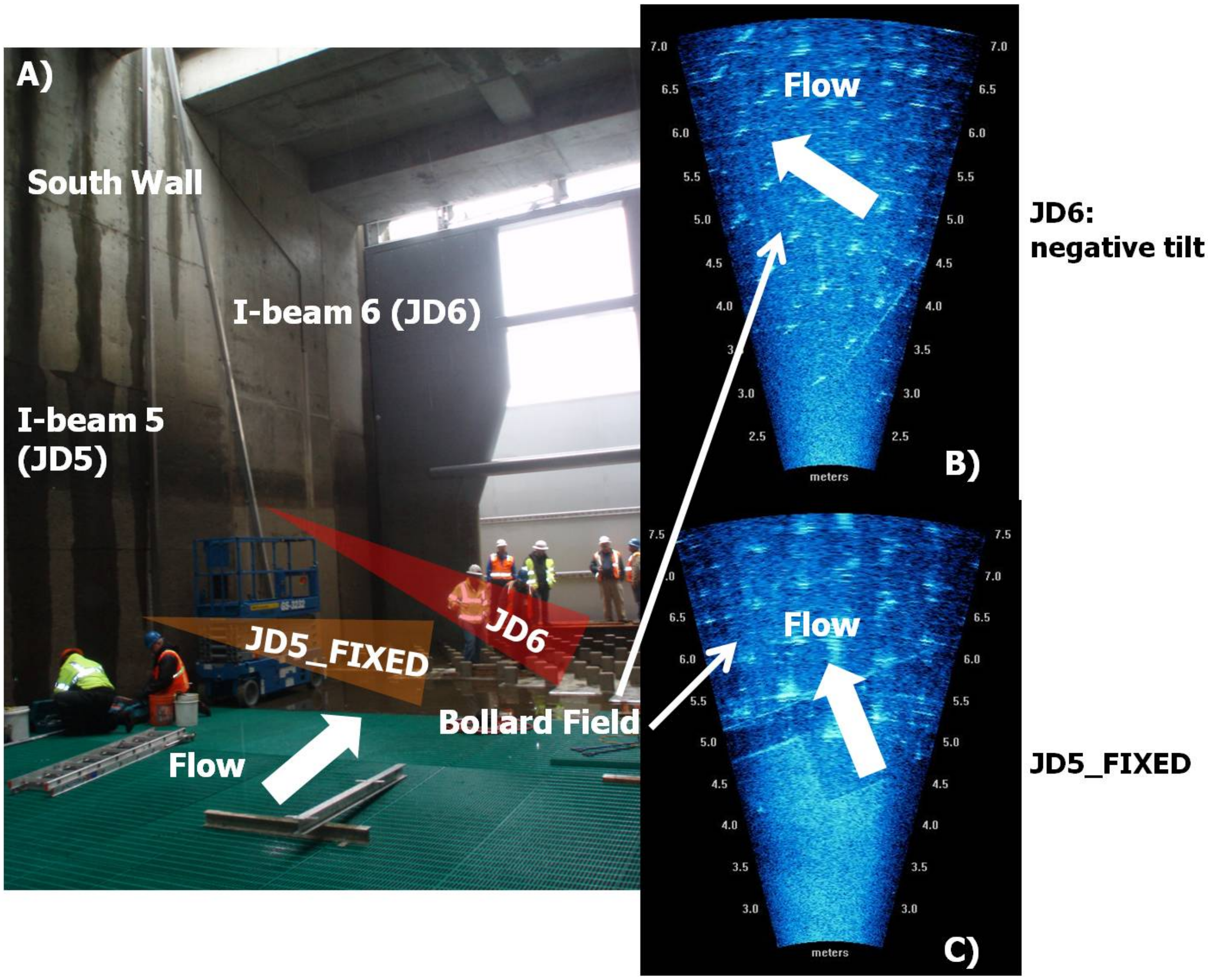

Figure 7. Deployment made at I-beam 5 (JD5) and I-beam (JD6) in 2013 at John Day Dam with DIDSON imagery capturing the inside of the bollard field for both (B) JD6 and (C) JD5_FIXED.

Figure 8. (A) DIDSON camera attached to the aluminum trolley at JD4 and (B) typical set up with the davit and protective workbox at John Day Dam.